Numerical and experimental evaluation of micromovements in an integrated system of bone fixation

Submitted in Partial Fulfilment of the Requirements for the Degree of Master in Mechanical Engineering in the speciality of Production and Project

Avaliação numérica e experimental de micromovimentos num sistema integrado de fixação óssea

Author
Diana Rodrigues de Almeida

Advisors
Professora Doutora Ana Paula Betencourt Martins Amaro
Engenheira Maria de Fátima de Costa Paulino

Jury

President	**Professora Doutora Maria Augusta Neto** **Professora Auxiliar da Universidade de Coimbra**
Vowel	**Professor Doutor Luis Manuel Ferreira Roseiro** **Professor Coordenador do Instituto Superior de Engenharia de Coimbra**
Advisor	**Engenheira Maria de Fátima da Costa Paulino** **Assistente Convidada da Universidade de Coimbra**

Coimbra, July, 2016

ACKNOWLEDGEMENTS

First of all, I have to thank both my parents and sister for all the unconditional support and care they gave me throughout my life. Their encouragement made it possible for me to believe in myself and follow my dreams.

I would like to thank my advisors, Professora Doutora Ana Amaro and Engineer Fátima Paulino for all the continuous support and guidance that was given to me. To Professor Doutor Luís Roseiro and Professora Doutora Maria Neto I also have to thank all the help and patience they provided me.

I also have to thank my friends and housemates for all the friendship and patience they gave me for the past years.

Last but not least, a great thank you to a very special person, André Travassos, for all the friendship, love, support and patience throughout the past five years.

Abstract

The bone stabilization to consolidate fractures is clinically used in medicine for quite a while. After World War II became necessary to develop mechanical systems that allowed stabilization of fractures of the limbs so that the bone could properly heal. Several types of fixator were developed throughout the years taking in consideration the severity of each situation, from trauma fractures to correction of bone deformities.

The process of bone regeneration and consolidation is fairly rapid in patients with some mobility as opposed to patients with poor or none mobility whatsoever. In these cases, stimulation of bone callus becomes a necessity in order to reduce the time of the fracture healing of the patient. Introducing micromovements into the fracture focus is the method of stimulation in which this dissertation inserts itself.

This work studies the possibility of engaging an engine to the frame of the fixator, enabling the transfer of micromovements into the fracture focus. Components are designed to support the engine to the frame and numerical models of the fixator are simulated to accomplish a relation between load applied in the nylon tube and its displacement. Furthermore, a methodology and experimental setup was developed with the purpose of analysing the value of load that is transferred to the fracture focus once considering an amount of stiffness that represents new bone callus.

Results are presented and discussed and continued work is suggested in order to accomplish an outcome that fulfils the aims of this dissertation's framework.

Keywords Bone Callus Formation, External fixator, Micromovements into the Fracture Focus, Limb lengthening, Osteotomy.

Resumo

A estabilização óssea para a consolidação de fraturas é utilizada pela medicina desde há muito tempo. Contudo, após a segunda guerra mundial assistiu-se a um crescimento no desenvolvimento de sistemas mecânicos direcionados para a estabilização de fraturas ósseas, em particular destinados à utilização em membros longos, de modo a permitir uma adequada cicatrização. Vários tipos de sistemas de fixação externa foram desenvolvidos ao longo dos anos, tendo em consideração a seriedade de cada situação, desde fraturas causadas de forma traumática a correção de deformidades ósseas.

O processo de regeneração e consolidação de osso em pacientes com alguma mobilidade é considerado rápido em oposição a pacientes com fraca ou praticamente nenhuma mobilidade. Para estes casos, a estimulação artificial do calo ósseo (osso regenerado) torna-se uma necessidade, não só para garantir o seu crescimento como para reduzir o tempo de recuperação do paciente. A introdução de micromovimentos no foco da fratura é uma forma de estimular a formação de calo ósseo e é este o enquadramento desta dissertação.

Este trabalho estuda a possibilidade de adicionar um motor ao fixador, permitindo a transferência de micromovimentos no foco da fratura. São desenvolvidos componentes com o objetivo de suportar o motor ao fixador e são utilizados modelos numéricos para a simulação da relação entre a carga aplicada no tubo de nylon e o deslocamento do mesmo. Para além disso, é desenvolvida uma metodologia com o objetivo de analisar o valor de carga que é transferida para o foco da fratura, ao considerar um elemento de rigidez variável que representasse novo calo ósseo.

Os resultados obtidos são apresentados e discutidos e são sugeridos alguns trabalhos de continuidade para completar os objetivos do enquadramento desta dissertação.

Palavras-chave:	Alongamento Ósseo, Fixador Externo, Formação de Calo Ósseo, Micromovimentos no Foco da Fractura, Osteotomia.

CONTENTS

LIST OF FIGURES

LIST OF TABLES

SIMBOLOGY AND ACRONYMS

Simbology

E – Young's Modulus;

F – Load applied in the tensile machine;

I – Moment of Inertia

K – Stiffness;

L – Length of the plate;

P – Value of force;

U – Displacement;

$dist_{axes}$ – Distance between the axis of the fixator beam and the nylon tubes;

x – Weight;

y – Value of microstrain of the strain gages.

Acronyms

ADINA – Automatic Dynamic Incremental Non-linear Analysis

ASTM – American Society for Testing and Materials

DEM – Departamento de Engenharia Mecânica

FCTUC – Faculdade de Ciências e Tecnologia da Universidade de Coimbra

ISEC – Instituto Superior de Engenharia de Coimbra

1. INTRODUCTION

1.1. Overview

Surrounding the World War II became necessary to develop mechanical systems that allowed stabilization of fractures of the limbs. The studies and applications were performed throughout the world, having contributed Belgian, Italian and American orthopedists to this progress. These mechanical systems were denominated as fixators with the purpose of fracture stabilization and to assure proper tissue regeneration.

However, external fixators are not only used in the case of bone fractures but also for limb lengthening. This is the case of some people that are born with congenital problems, namely dwarfism condition, and the treatment usually involves the bone osteotomy and only after the stabilization of the fracture with a fixator. To assure limb lengthening it is necessary to stimulate new bone formation. The main objective of this dissertation is to study the possibility of artificially introduce micromovements into the fracture focus, with an engine, to promote new bone formation. The micromovements in the fracture focus have been studied by some authors and it is general consensus that controlled and axial micromovement, being applied a few weeks after osteotomy, has benefits, regarding callus formation and faster healing time of the patient.

The framework of this dissertation inserts itself on the development of mechanical systems allowing the introduction of micromovements into the fracture focus of the tibia, therefore, enhancing bone callus formation and enabling faster healing recovery of the patient. Having in mind patients with near to zero mobility, this dissertation will hopefully has an impact on quality of life of the patient through improvements on the course of treatment.

The methodology used on this study makes use of a simplified tibia, consisting on two nylon beams, an Orthofix® external fixator and a developed mechanical system made with two instrumented Carbon Epoxy Laminated Composite beams, in order to measure the force through de simplified tibia. Throughout this dissertation, numerical simulations and experimental work were performed with distinctive purposes. A methodology was

developed in order to study the amount of load that is transferred into the fracture focus, once there is a load being applied in the tibia. To analyse the influence that weight bearing of the patient's tibia has on the displacement and, consequently, on the free clamp of the fixator, models were simulated in the commercial software ADINA®.

1.2. Aims

The purpose of this dissertation is to study the mechanical behaviour of an external fixator's frame when being solicited under compression, and to be able to determine the amount of load that passes through the fracture focus, when the tibia is being solicited. This work also has the aim to study the possibility of adding an engine to the external fixator, enabling the transfer of micromovements into the fracture focus.

1.3. Outline

The structure of this dissertation is divided into six different sections, the first being a brief introduction enhancing the goals and relevance of this work. Chapter 2 presents the literature review necessary to the study and comprehension of some important concepts of this dissertation, namely the types of external fixators and its application on the regeneration of bone, focusing on improvements to the callus stimulation. Chapter 3 presents the methodology that was implemented in order to study the mechanical behaviour of the external fixator engaging an element of variable stiffness, whereas Chapter 4 presents the numerical study of the external fixator having engaged a spindle drive. The results obtained regarding these two previous chapters are analysed and discussed in Chapter 5, the conclusions and final considerations of this dissertation are presented in Chapter 6.

2. LITERATURE REVIEW

The present chapter of this dissertation introduces the concept of external bone fixators as a resource to achieve safe and faster healing of tibia fractures.

This chapter is divided in five sections. Section 2.1 describes the anatomy of the bone, distinguishing the trabecular from the cortical bone and enouncing its mechanical properties according to some researchers. Section 2.2 refers to the different types of fractures, particularly in the diaphysis of long bone members and the suitable treatment that should be prescribed, in order to minimize the healing time necessary to restore maximum or total mobility of patients. Section 2.3 presents a brief introduction to the use of external fixators, but also a summary of the types of fixators being developed throughout the years, the terminology that it still being applied nowadays as well as some components used in the frames. Section 2.4 is dedicated to bone regeneration and bone callus stimulation.

2.1. Anatomy of the bone

The human skeleton of an adult body has in its constitution 206 individual bones which are arranged in two different areas: the axial skeleton, in which there are 80 bones in some regions surrounding the upper body such as the skull, the sternum and vertebral column, and the appendicular skeleton composed of 126 bones in the upper and lower limbs [1]. Long bones, such as the tibia and the femur, have in its constitution two very distinctive areas: the diaphysis, which is composed mainly of compact bone but there is also a small portion of spongy bone, and the epiphysis which is mainly made of spongy bone [1][2].

Referring to the lower limbs, the structure of the bone is composed of two different materials, the cortical bone and the trabecular bone, as represented in Figure 2.1. The trabecular bone, being in the inner part of the bone, is known to be very porous and is frequently designed as spongy bone, whereas the cortical bone, which forms the outer area of the bone, is much denser and stiffer [2][3].
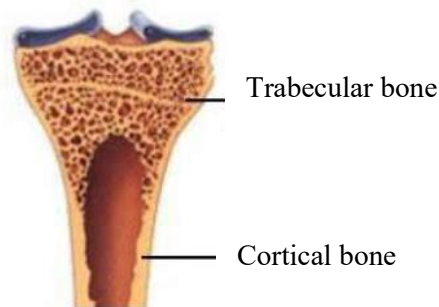
Figure 2.1. Bone material [2].

In 1996 Lowet *et al.* [4] studied the vibrational behaviour of a tibia by developing a finite element method in which the properties of bone material that was used were similar to the ones referred by Hobatho *et al.* [5], used in 1991. These mechanical properties, considered on this study are presented in Table 2.1 [4].

Table 2.1. Properties of the bone [4].

Property	Epiphysis	Diaphysis
Density	300 kg/m^3	1800 kg/m^3
Young's modulus	1.1 GPa	15 GPa
Poisson's ratio	0.33	0.33

2.2. Fractures and suitable treatments

The bones, while being very stiff, can still break during an unexpected injury and its severity usually depends on the amount of energy that caused the bone to break. In order to choose the suitable treatment it is important to evaluate the type of fracture that occurred. The present work will have an emphasis on the diaphysis fractures.

According to "Müller AO Classification of Fractures – Long bones" [6], if the fracture separates the bones into two parts, it can be described as a simple fracture whereas if the bone were to be divided into more than two parts, it would be considered a multi-

fragmentary one. In this case, if there is contact between the fracture ends, it is a wedge fracture otherwise it is a complex one. Figure 2.2 presents a brief distinction of types of fractures divided according to its severity. If the skin gets damaged and perforated by the bone, it is considered an open or an exposed fracture.
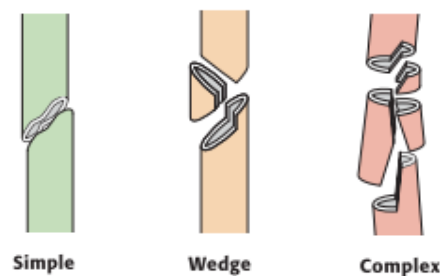
Figure 2.2. Classification of fractures of the diaphysis into the three fractures groups [6].

There are a number of treatments that can be applied to the patient after a fracture. However, to decide the treatment direction, the orthopedist needs to analyse each case differently, taking into consideration some aspects like the age of the patient, whether or not the injury is life-threatening, the patient's occupation and lifestyle [7]. The most commonly methods for treatment of fractures include [2]:

- o Cast immobilization – applying cast in the area of the fracture to stabilize it.
- o Internal fixation – bone fragments are repositioned and stabilized through bolts and plates placed on the bone external surface.
- o External fixation – a number of pins perforate the bone above and below the fracture and connect to an external frame, stabilizing the fracture.
- o Traction – usually used to align bone fragments.

When a bone fracture occurs it is imperative to stabilize it, usually through some method of bone fixator. These fixators enable fast healing of the injured bone and allow to return early mobility to the patient. The type of fixator used could be internal or external. Internal fixation has been used since the late 1950s when in need of restoring bone anatomy and its main goal is being able to achieve full function of the injured bone, whereas external fixators enable the surgeon to control the flexibility of the fixation and are standard

procedure when necessary to avoid damage to an already injured limb [8]. The present dissertation has a focus on the use of external fixators as a treatment method.

2.3. External fixators

The method of external fixation is primarily used for trauma purposes and deformity corrections, with the main purpose of bone realignment. Based on the principle of splinting, the advantages associated with external fixation include simplicity and adjustability of the fixator. [9] However, bone fixation took upon several developments along the years. This method of treatment began to take place during the 19th century with Jean Francois Malgaigne who developed a claw-like clamp with the intention of reducing and stabilizing fractures, as seen in Figure 2.3 [2][3][10].
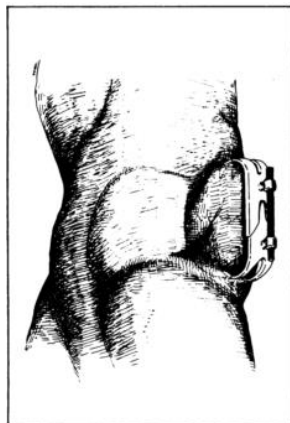
Figure 2.3. Claw-like clamp (Malgaigne, 1843) [10].

In the late 19th Century, both the American Clayton Parkhill and the Belgian Albin Lambotte developed a system that is quite similar to those that are currently used in orthopaedics, being a system that harbours a rigid external plate connected with pins. It is important to emphasise that exchanging information was nearly impossible at that time and it was a coincidence that both researchers reached the same conclusion in their work. In Figure 2.4. it is possible to visualize the schematics of the systems that both Parkhill and Lambotte designed [3][10].
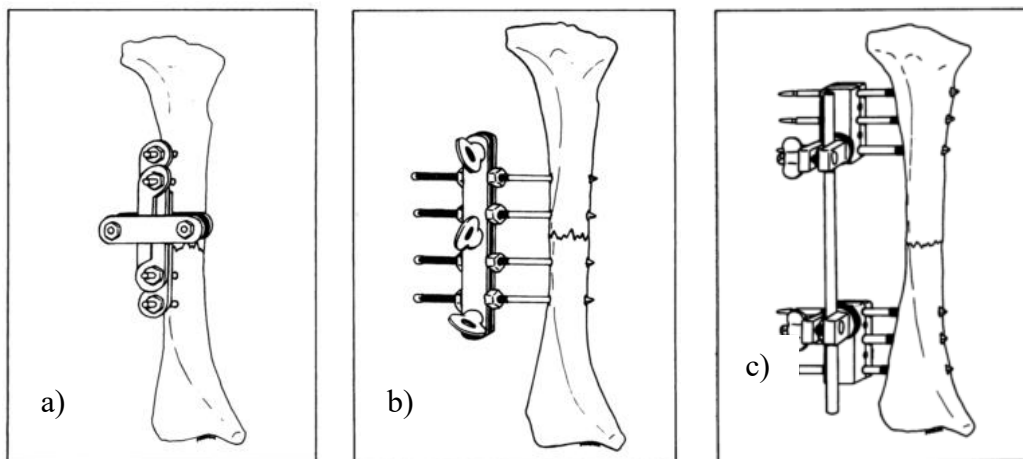
Figure 2.4. a) Parkhill's bone clamp; b) Lambotte's external fixator; c) Hoffman's frame [10].

In Europe, during the 20th Century, many surgeons took upon Lambotte's original concept of external fixator, and expanded on it. Particularly Raoul Hoffman who, around 1938, devised a unilateral fixator that included an adjustable sliding system to reduce fractures, schematized in Figure 2.4.c) [3][10]. These fixators were considered unilateral, having the frame one-sided.

According to W. R. Pontarelli [10], towards the end of World War II, military surgeons documented significant complications regarding the use of external skeletal fixation. The Committee on Fracture and Trauma Surgery of the American Academy of Orthopaedic Surgeons, after investigating the use of these fixators, noted several advantages such as stable fixation and reduced hospitalization. However, significant disadvantages were also noted namely infections or delayed union. As such, many surgeons without the proper expertise were advised against performing this procedure.

Gavril Ilizarov [11] has revolutionized the treatment of orthopedic conditions during the 20th Century. He stated a few principles as key to get faster healing time, namely having stable fixation, functional activity of the muscles and joints and early mobilizing the injured patient. Thus, the Ilizarov circular fixator frame was developed and clinically used.

The Ilizarov frame is a set of mechanical components consisting of rings, rods and kirschner wires, all made by AISI 316 L stainless steel. This type of fixator can be seen in Figure 2.5. The main difference from the conventional external fixator is that it supports the limb as a cylinder and provides greater support than the one sided fixators. The purpose of the Ilizarov fixator is to stimulate bone growth, through the principle of distraction

osteogenesis which consists on pulling apart the limbs to stimulate new bone growth [11]. Even though the original circular frame designed by Ilizarov was developed for limb lengthening, it was recognized that in other orthopaedic situations, this treatment was also very effective [12]. The concept of distraction osteogenesis was then studied through the application of several other types of external fixators throughout the years [2].
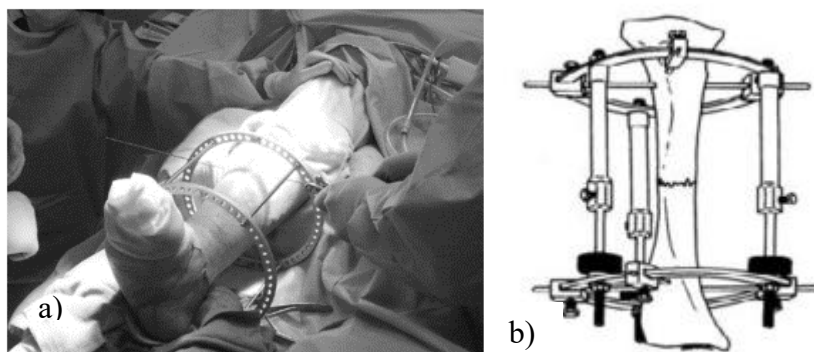
Figure 2.5. a) The Ilizarov frame. [12]; b) Schematics of the Ilizarov frame [3].

According to Taljanovic et al.[8], there are three types of external fixators, namely the standard pin fixator, the ring fixator and the hybrid fixator. The standard pin fixator consists on thoroughly placed pins connected to an external rod and can be used in almost every long bone fracture. The ring fixator is a technique that was first introduced by Ilizarov with the purpose of limb lengthening procedures. These fixators are made of thin wires under tension that are linked to circular or semi-circular frames. The hybrid fixator, being represented in Figure 2.6, consists on a combination of both ring and standard uniplanar fixators and it is usually applied when treating fractures that are close to the joint.

Figure 2.6. Example of a hybrid fixator [13].

External fixators are adjustable mechanical systems and there were developed several combinations of linear fixators throughout the years. The terminology normally used to classify the external fixators can be defined [10]:

o Unilateral: this frame employs one bar or rod, on one side of the limb, connected to the bone by, at least two pins;

o Bilateral: this frame uses fixators on two parallel sides of a limb;

o Biplanar: the bars are place in two or more planes for added stability.

These three types of external fixators are shown in Figure 2.7.
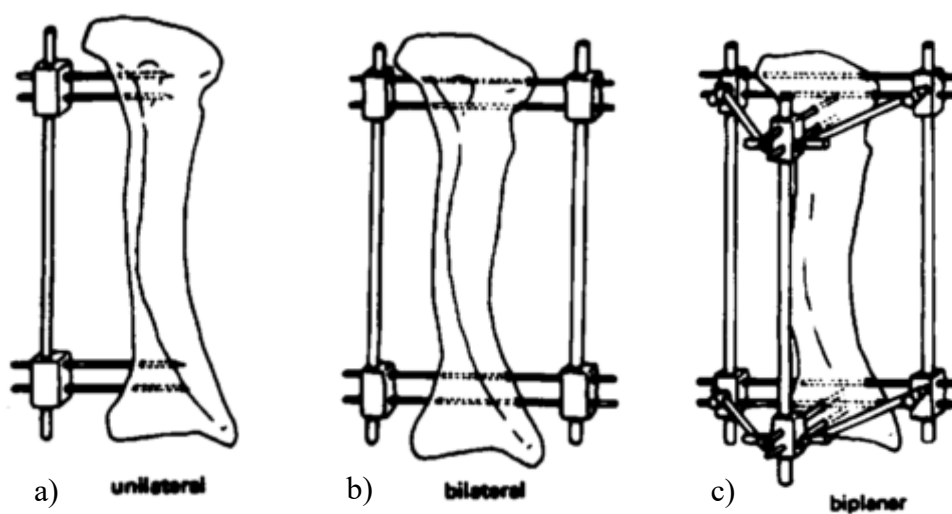
Figure 2.7. Types of configurations of linear external fixators: a) unilateral; b) bilateral; c) biplanar [10].

After the decision of the orthopedist concerning the use of an external fixator as the best course of treatment for the patient, it is very important to stabilize the bone structure early. Normally the frames are of easily construction and very adjustable, consisting of pins or wires, clamps, bars or rings, which can be used to form all different types of external fixators. The pins and wires are essential to guarantee the stability of the frame.

The most commonly used pins and wires are the Schanz and Steinman pins, as seen in Figure 2.8, and the Kirschner wires. Whereas the Schanz pins have a threaded end to allow fixation on the trabecular bone, the Steinman pins have a bevelled end and sometimes a threaded section in the middle to guarantee better fixation [2][9]. The diameter is usually between 2 and 6 mm for both these pins. The Kirschner wires are used alone or as a component of an external fixator, like the Ilizarov fixator. They are commonly used in circular or hybrid frames [2].

Figure 2.8. a) Schanz pins; b) Steinman pins [3].

According to Moss *et al.* [9], when decided to place an external fixator, preoperative planning is essential due to the feasibility of contamination of the wound of the injured patient. It is essential to maximize the structure stiffness, however adding pins to the frame can increase the possibility of infection. A technique that is most used is the application of four pins into the frame being that two pins should be located as close to the fracture and the other two as far away as possible. [9]

2.4. Bone regeneration

Bone tissues have the capacity to regenerate as an answer to injury or under continuous remodelling throughout the adult life. During fracture healing, new bone is formed and continuously remodelled until its mechanical properties are restored, normally through primary or secondary healing [14]. Whereas primary healing involves direct cortical remodelling without any callus (external tissue) formation, secondary healing occurs when interfragmentary movement between the edges of the fractured bone is present, and it is the process by which most fractures heal naturally [14][15].

Bone repair by secondary healing generally occurs through a tissue differentiation process, going from an initial hematoma or blood cloth, to stages of soft and hard callus formation and external bony bridging and finally bone remodelling, as seen in Figure 2.9. [14][15].
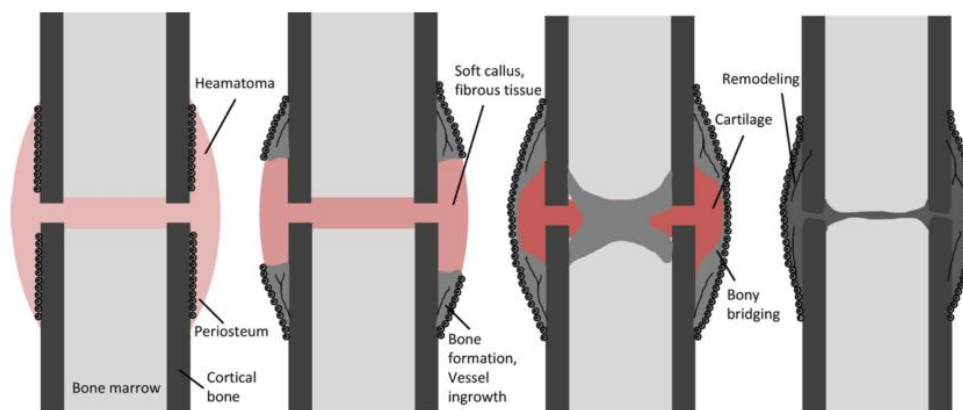
Figure 2.9. Schematics of secondary bone fracture healing [14].

People born with congenital problems, like dwarfism conditions or other birth defects may suffer several medical problems. In this case, it is very common to induce fracture in order to lengthen the lower limbs. This process initiates with a bone osteotomy, which is the surgical cut of the bone, and then an external or internal device is placed in order to assure fracture stability. Afterwards, new bone is formed, usually through some kind of stimulation [3][16].

2.4.1. Callus stimulation

Mechanical loads promote deformation of the bone which leads to bone resorption and increase in new bone formation thus increasing the strength of the bone. This explains the reason why mechanical stimulus is so important in promoting bone growth and remodelling. Callus formation can also be stimulated by the following processes [17]:

- o Electric stimuli – alternative method of fracture healing without the need of surgery;
- o Laser stimuli – laser therapy of low intensity (helium-neon) is beneficial in bone remodelling;
- o Stimuli by ultrasound - the ultrasound propagates through high frequency acoustic waves that promote micro-deformation thus accelerating bone growth;
- o Stimuli through walking – increasing the load that is applied in the lower limbs, through walking, induces a local bone response that allows bone growth and remodelling.

Mechanical environment has influence in the pattern of fracture healing. In cases of the patient being immobile, the stimulation can be promoted by applying cyclic micromovements. These micromovements are being schematized in Figure 2.10. Several authors have studied and published papers with the aim to accelerate fracture healing and reducing the patient's recovery time thus improving quality of life.
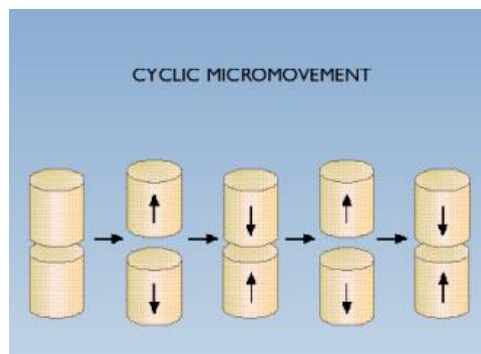
Figure 2.10. Schematics of cyclic micromovements applied in the fracture focus [18].

Goodship and Kenwright [19] promoted a maximum axial displacement of 1 mm with a constant force of 360 N being applied in a frequency of 0.5 Hz. They associated the improvement of fracture healing when applying controlled micromovement to the fracture focus.

Ilizarov *et al*. [20] evaluated the optimum conditions for bone growth during limb lengthening on the canine tibia using the Ilizarov circular external fixator and obtained better results with a distraction rate of 1.0 mm per day.

Gardner *et al*. [21] studied the influence of external fixators on fracture motion during simulated walking. They considered four directions of interfragmentary motion in the simulation: transverse shear, axial, angular and torsional shear. The axial motion is the one which has the more influence on callus formation and they concluded that each 60 N of axial load promotes 1.0 mm of compression in the fracture.

Later, Yamaji *et al*. [22] published a study that aimed to identify the suitable amount of micromovement to promote callus formation and bridging of the bony fragments on successful fracture healings. Their experiments were made on sheep's, dividing them into groups with different gap sizes and micromovements. They concluded that a large gap between the edges of the bone fracture delays the healing process.

Kenwright *et al.* [23] attached a pneumatic plump to an external fixator in order to allow axial movement in some short periods of the day. Until the patient regained mobility, they were submitted to movements at 0.5 Hz, during 20 minutes a day which lead to an axial movement of 1.0 mm. They noted that applying early movement has a beneficial influence upon fracture healing.

In 1998, Wolf *et al*. [24] published a study with the sole purpose of investigating the mechanical stimulus on fracture healing under flexible fixation resourcing several sheep within the weight of 50-60 kg. The mechanical stimulation began 12 days after the osteotomy procedure and it was applied during 20 minute a day (1200 cycles at 1 Hz). Loading was applied at a rate of 2 mm per minute for axial loads and bending loads and 2° per minute for torsional loads. An electromechanically driven module enabled the axial micromovement when attached to the fixator, as seen in Figure 2.11.
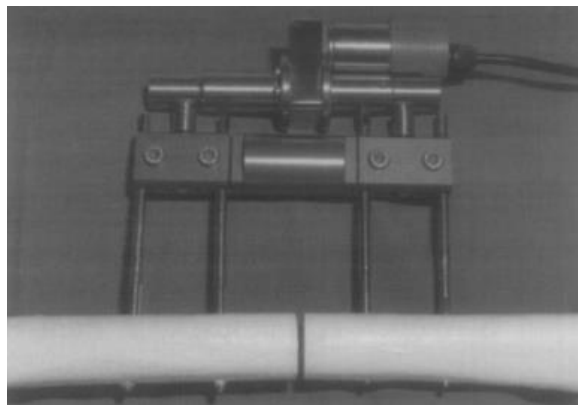
Figure 2.11. Micromovement module applied to the external fixator [24].

3. SETUP ENGAGING AN ELEMENT OF VARIABLE STIFFNESS

Knowing the influence that the weight bearing of the patient has on the stimulation of the callus growth can potentially aid in reducing its healing time, thus improving quality of life to the patient. This chapter initiates with the presentation of the external fixator. Section 3.3 is dedicated to the methodology used to develop an experimental setup with the purpose of studying the behaviour of the external fixator, specifically, to quantify the amount of loading that the frame could absorb, when solicited.

3.1. External Fixator Orthofix® LRS

The external fixator Orthofix Limb Reconstruction System (LRS) is recommended for patients with short stature, to treat open fractures and angular deformities. The 3D model in Figure 3.1 represents the model in which modifications will be made in order to maximize its potential according to the aims of this dissertation. In order to simulate the behaviour and properties of the tibia, two nylon tubes 200 mm long were machined and, in each tube, two Schanz pins of 6 mm of diameter were connected.
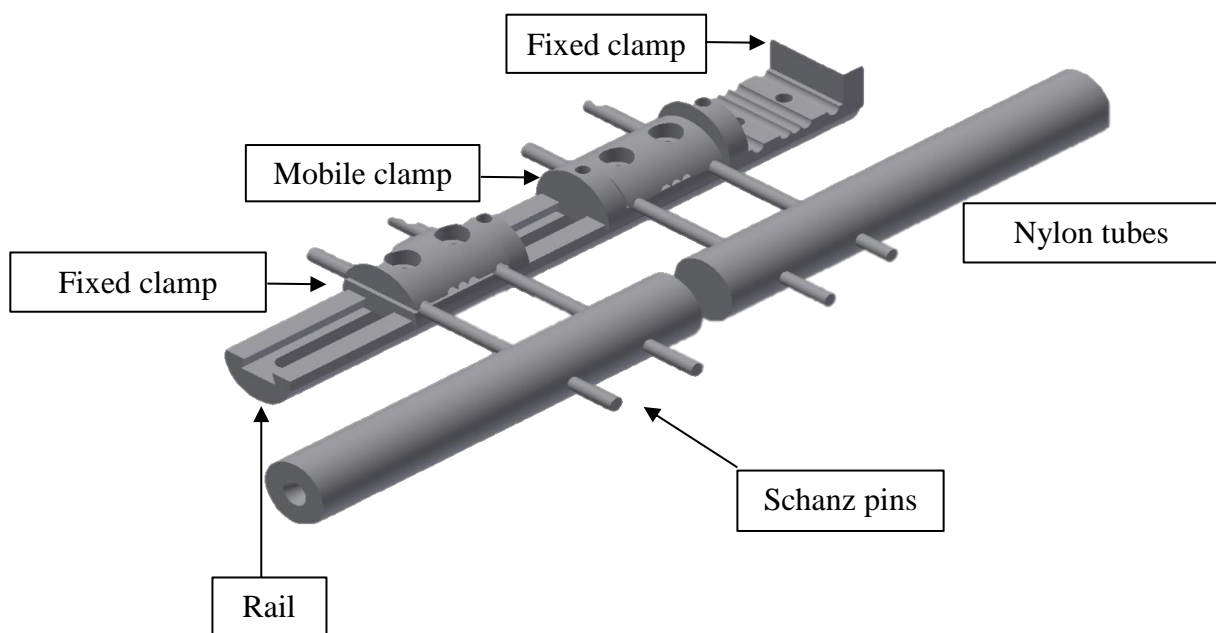
Figure 3.1. 3D Model of the frame of the external fixator.

3.2. Optimization of the value of stiffness of the spring

The work previously done by Paulino *et al.* [24] considered a setup that engaged a structural element of variable and adjustable stiffness. The setup included a Sawbones® tibia with a 4 mm fracture central area of the diaphysis, an Orthofix® external fixator, with 80 mm distance from bone axis to fixator beam, three pins on each side of the fractured bone, and an added element group with variable stiffness, guaranteed by a spring. They implemented a methodology that allowed the optimization of the value of stiffness of the spring in order to achieve a displacement of 1 mm and they reached the value of 640 N/mm. This stiffness value was obtained considering that both the pins and the external fixator, were made with steel AISI 316L. Later on, the value of optimized stiffness was updated considering the fixator as Aluminium Alloy 7075 T6, reaching a value of stiffness of 1400 N/mm.

3.3. Value of load in the fracture focus

One of the aims of the present work is to evaluate the value of load that passes through the fracture focus. When there is a load being applied in the nylon tube, which represents the weight of the patient, only a part of it goes through the nylon into the fracture focus due to the load being absorbed by the frame of the fixator, as can be seen schematically in Figure 3.2. So it became important to quantify the load that, realistically, passes through the tibia. An experimental setup including strain gages glued to a surface was developed. The goal was to use the strain gages as a load cell allowing the determination of deformation of the plate's surface, when there was load being applied in the nylon tube, thus obtaining the value of load in the fracture focus.
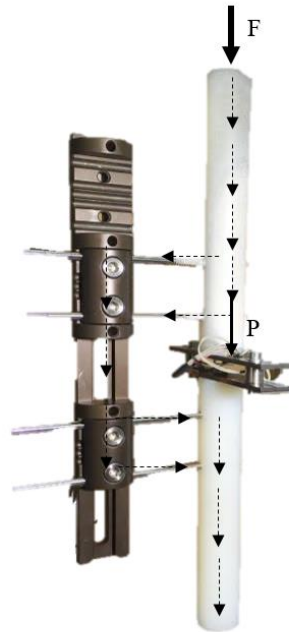
Figure 3.2. Schematics of the distibution of load throughout the external fixator.

3.3.1.   Load cell components and procedure

As can be seen schematically in Figure 3.3, the developed load cell is based on two parallel rigid plates connected by two circular supports.
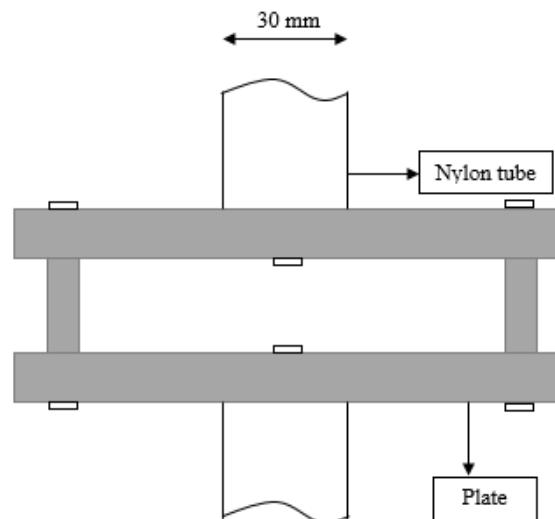
Figure 3.3. Load cell schematics.

Firstly, it was necessary to reach a conclusion as to which material to use as plates and the distance between the supports. Four different materials were thought to use as plates, however, the global stiffness need to be similar to the values of stiffness that had been previously optimized of 640 N/mm and 1400 N/mm. By having different distances between supports in the same plate, different values of stiffness could be obtained.

The commercial finite element program ADINA allowed to proceed with the comparison between different materials: Aluminium Alloy, Carbon Epoxy Composite, Steel Alloy and Fiberglass, where the displacement was also taken in account. The numerical simulation was simplified with an isotropic material and the type of element used was a Beam with six elements. The value of displacement of the y-axis was obtained in the central node of the plate's length and compared with the analytic calculation. These values are presented in Table 3.2. The equation (3.1) allowed the determination of the value of displacement in the central section of the plate, in which P is the value of load applied in the plate, L is the length of the plate, E is the Young's modulus and I the moment of inertia. In this numerical simulation both supports were fixed and the force applied in the central node was of 300 N.

$$U = \frac{PL^3}{192EI}$$ (3.1)

Referring to the rigidity, whereas the Fiberglass lacked in stiffness, the Steel Alloy was too stiff. Considering the Aluminium Alloy, there can be some difficulty associated with the collage of the strain gages. Thus, the Carbon Epoxy Composite with distance between supports of 100 mm and 130 mm was ideal to achieve the optimized stiffness, as represented also in Table 3.2. Notice that the value of displacement of the composite plate with the imposed stiffness is different than 1 mm due to the different conditions that were promoted in Paulino *et al*. [24], namely the number and position of pins that were used in their work. The value of stiffness of these materials was calculated from the equation (3.2).

$$K = \frac{EI}{3L^3}$$ (3.2)

Table 3.2 Characteristics of the chosen material for the plates.

Material	Carbon Epoxy Composite	
Young's Modulus [GPa]	102	
Distance between supports [mm]	100	130
Dimensions of the plate [mm]x[mm]	20 x 3.5	
Length of the plate [mm]	150	
Y-Displacement [mm]	0.214	0.471
Stiffness K [N/mm]	1400	640
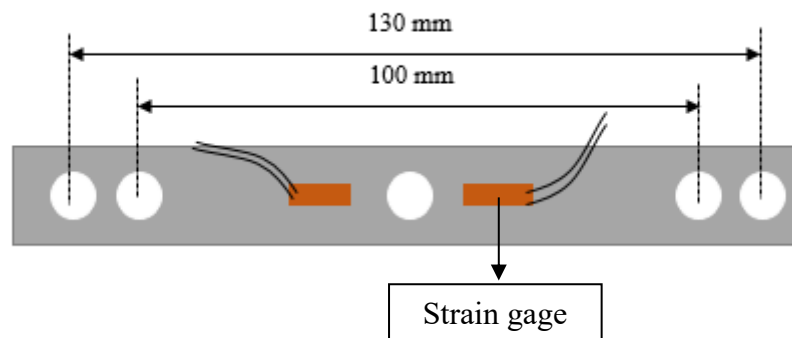
Figure 3.4. Schematics of the Composite plate with the selected lengths.

3.3.2. Strain gages considered

Four strain gages were used to obtain the load cell. The strain gages were from Vishay Micromeasurements, having the following reference: CEA-06-125UN-120 with a grid resistance in ohms of $120 \pm 0.3\%$ and a gage factor of $2.085 \pm 0.5\%$ at 24ºC. In Figure 3.5 it is possible to observe a strain gage glued in the composite plate with its terminals.

The positioning and collage of the strain gages went through the following methodology:

1) The composite surface was degreased and cleaned by applying an acid solution to attack the surface followed by a basic solution to neutralize it;

2) The lines necessary to guide the collage of strain gage were marked on the composite with a pencil;

3) The surface was cleaned once more;

4) The strain gage and its terminals were carefully arranged on a previously cleaned acrylic surface and a non-reactive adhesive tape was applied on top of them;

5) The adhesive tape with the strain gage was carefully placed on the composite surface with its terminals arranged with the pencil markings. Afterwards, by lifting an extremity of the adhesive tape, it was able to apply the cyanoacrylate glue under the strain gage. To assure better adherence, a finger was pressed on top of the adhesive tape during 30 seconds;

6) The adhesive tape was lifted. Another adhesive tape was glued to the strain gage only leaving the terminals uncovered;

7) The conductor wires were welded to the terminals;

8) This methodology was followed for all four strain gages.

Figure 3.5. Strain gages glued to the composite plate.

Two strain gages were glued to the bottom of the top plate, also referred as plate A, and other two strain gages were glued to the bottom of the lower plate, also called plate B. The strain gages were connected to a P3 Vishay Micromeasurements box (Wheastone bridge), which enables the record of the data into a file. Taken into account the defined position of the strain gages in the two plates (two with positive deformation and two with negative deformation), any type of bridge connection can be considered, namely full bridge, half-bridge or quarter bridge.

Due to manufacture conditions, and in order to avoid eventually problems of delamination between one or more strain gages and the plate, the option considered in this

work was the connection in four quarter bridge. With this option four deformation data can be used to calibrate the load cell. This equipment can be seen in Figure 3.6.
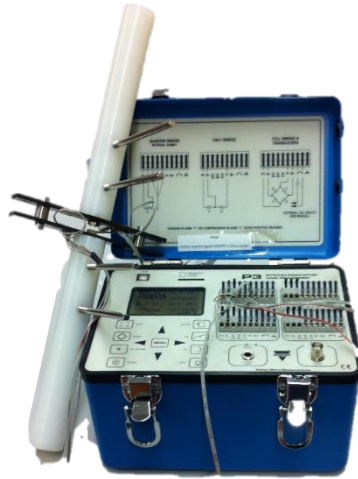
Figure 3.6. Strain gages connected to a P3 Vishay Micromeasurements.

3.3.3. Methodology of the calibration procedure

The experiments used to obtain the calibration of the load cell were made in Applied Mechanics Laboratory from ISEC.

The calibration was performed with a distance between supports of 100 mm. Firstly it was performed a calibration in which the frame was solicited under traction and only afterwards under compression. The four set of wires were connected to the Strain Indicator and Recorder by Vishay Micromeasurements.

The set of wires denominated as "A" were connected to channel 1, the set of wires "B" to channel 2, "C" to channel 3 and "D" to channel 4. The wires "A" and "B" were solicited under compression due to being connected to the strain gages of plate "A" and the set of wires "C" and "D" under traction due to being connected to the strain gages in plate "B".

The procedure to obtain the calibration followed as such and was made considering both the amount and descend of applied weight:

1) The setup was arranged in the embroidery frame and five calibrated weights of 20 N were selected. The first tests were performed with the setup under traction, as seen in Figure 3.7.a);

2) With the P3 Strain Indicator and Recorder connected to a laptop, the quarter bridge option was selected and the value of the gage factor was defined. The device was set to zero and then the first reading of the strain gage was registered;

3) The calibrated weights were placed on the setup one by one and within each weight the deformation of the strain gages were measured. After having placed 100 N, the weights were carefully removed one by one, always measuring the value of deformation between each weight;

4) After repeating this procedure three times, the setup was removed and arranged differently in the embroidery frame so that the following three evaluations were performed under compression, Figure 3.7.b) and c). The procedure with the calibrated weights was the same as described above.
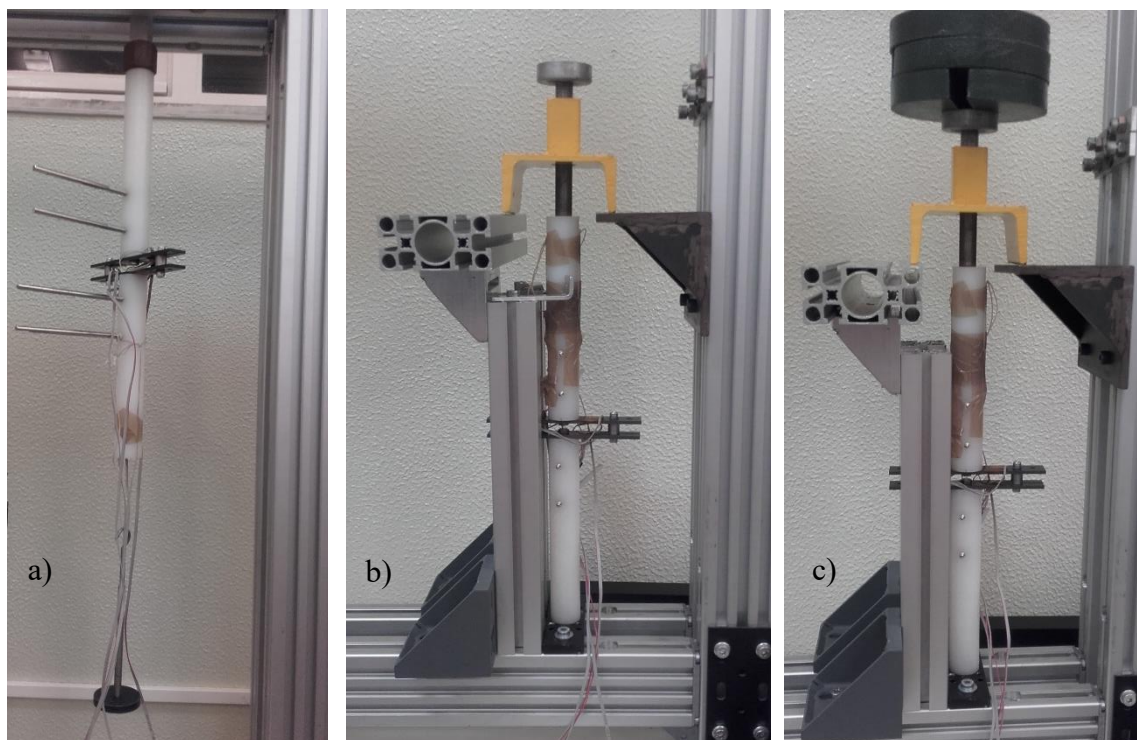
Figure 3.7. Setups with the intent of calibration. a) traction setup; b) compression setup; c) compression setup with three weights of 20 N.

3.4. Experimental Tests with a Tensile Machine

Tensile testing is the fundamental type of mechanical test to perform on a material with the purpose of understanding how the material will react to forces being applied in tension. It is a destructive test that allows to define some material's mechanical properties such as the modulus of elasticity, the Poisson's ratio and the tensile strength. In this case, a tensile machine, SHIMADZU model AUTOGRAPH AG-X in DEM-FCTUC, was perform the experimental tests, namely to apply and register the controlled force and/or displacement.

The mechanical system consisting on the frame of the fixator, the strain gages and the nylon tubes was placed in the tensile machine. The tensile machine is connected to a computer to warrant the use of its own software "TRAPEZIUM X" to register the test results, consisting on the evolution of the applied load with the value of displacement. The software of the tensile test enables the fixation of the displacement or the maximum value of attainable load. In these tests, the maximum displacement was fixed to a value of 1 mm and the tensile tests were made with a velocity of 2 mm per minute, in order to analyse the value of load that promoted a displacement of 1 mm.

The aim of the tensile test was to analyse the data obtained by the strain gages during the tests, which represents the load in the artificial fracture focus, having the nylon tube being solicited under compression. The setup can be seen in Figure 3.8. The tensile test was performed taking in consideration the specifications described in norm ASTM F 1541 – 02 [25].

The experiment was performed considering two different lengths in the plates of the developed load cell and consequently different amounts of stiffness, namely the 100 mm and 130 mm, explained in Section 3.3.1. In the experimental setup, the distance between the axis of the frame and the centre of the nylon was also varied, being 50 mm, 60 mm, 70 mm, 80 mm, 90 mm and 100 mm. This distance between axes is schematized in Figure 3.9. The test was performed for these different distances with the purpose of studying the sensibility of the position of the external fixator on the amount of load that is absorbed by.
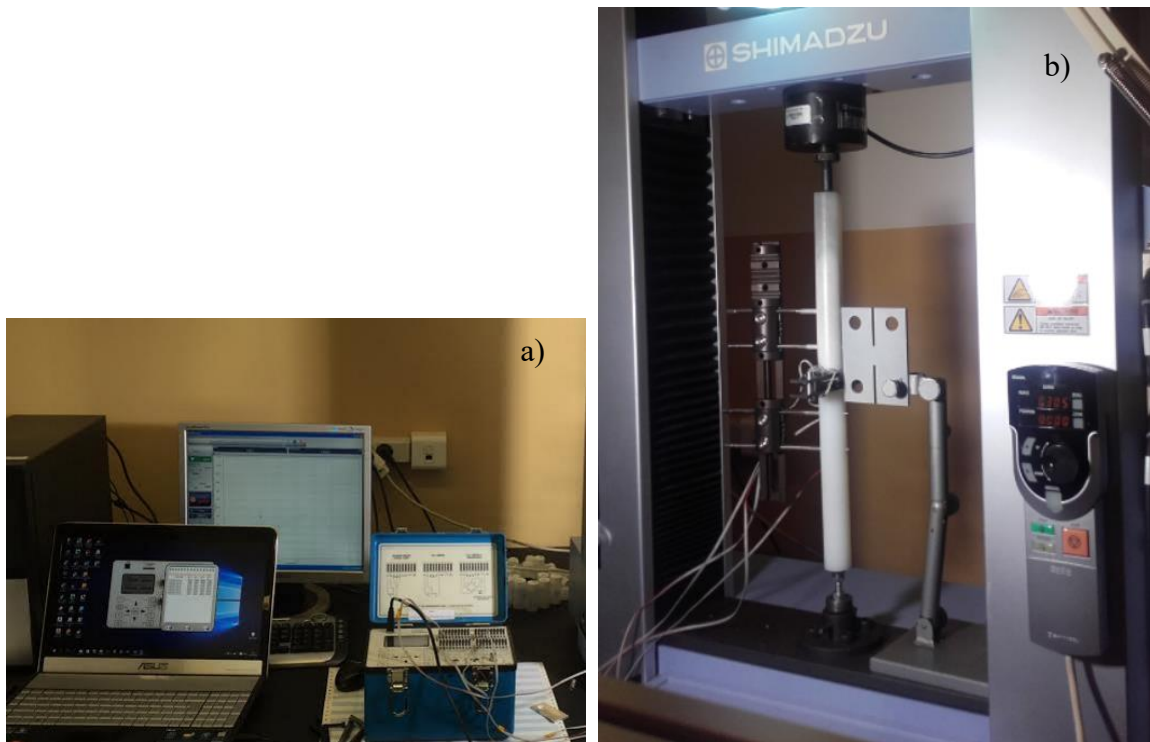
Figure 3.8. a) Experimental setup; b) Test perfomed in the tensile machine the with a distance between axes of 50 mm.
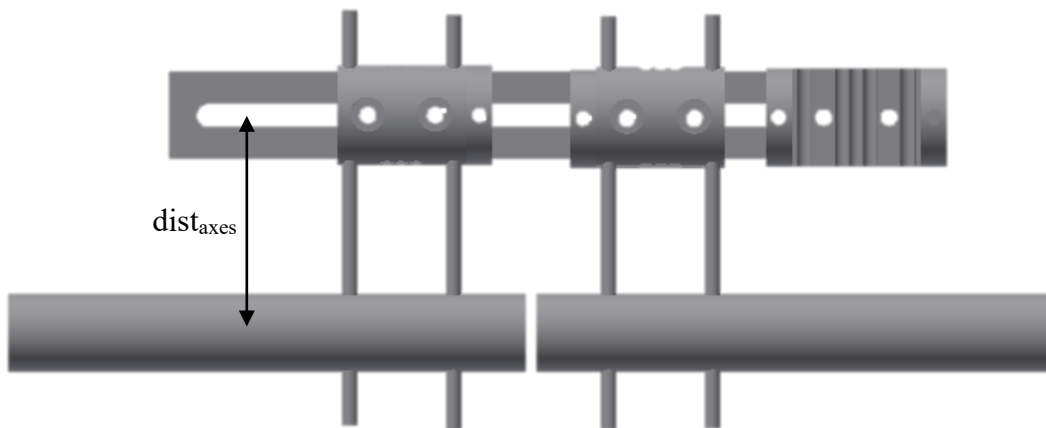
Figure 3.9. Model of the setup schematizing the distance between the axes of the fixator's beam and the nylon tubes.

4. SETUP ENGAGING A SPINDLE DRIVE

As presented in section 1, one of the aims of this dissertation is to introduce a device that promotes micromovements to the fracture focus in order to reduce the healing time of the patient. To achieve this goal with an engine, it became necessary to develop some mechanical components that enables the support of the device to the frame of the fixator.

This chapter is divided in four sections. In the first section is presented the selected spindle drive. In the second section is presented a number of components designed to support the engine and the respective parameters to numerically analyse the structure. Section 4.3 is reserved to the improvement of these components and its numerical study. Finally, section 4.4 is dedicated to the validation of the tensile test.

4.1. Spindle drive

The spindle drive that was ordered online to fulfil one of the purposes of the present dissertation was a Spindle Drive GP 16 S. This spindle, along with a DC motor, will allow to transform rotary motion into axial motion. Figure 4.1 represents the spindle drive that will be used and its specifications are presented in Annex A.

Figure 4.1. Spindle drive GP 16 S.

4.2. First components

As referred above, this section concerns the development and design of components with the purpose of adding an engine to the frame of the external fixator. These components were designed in the software Autodesk Inventor Professional 2016.

A safety clamp, identified in Figure 4.2 as part B, was included in the frame to prevent unexpected axial movements in case of engine malfunction, assuring the safety of the stability of the frame during treatment. The initial idea for the support was that the spindle could be secured in one of its extremities by a support clamp which was connected through one or more bolts to a clamp fixed to the rail, as seen in Figure 4.3. The component A in Figure 4.2 was threaded and connected to the nut and was also connected to the mobile clamp, as identified in Chapter 3.
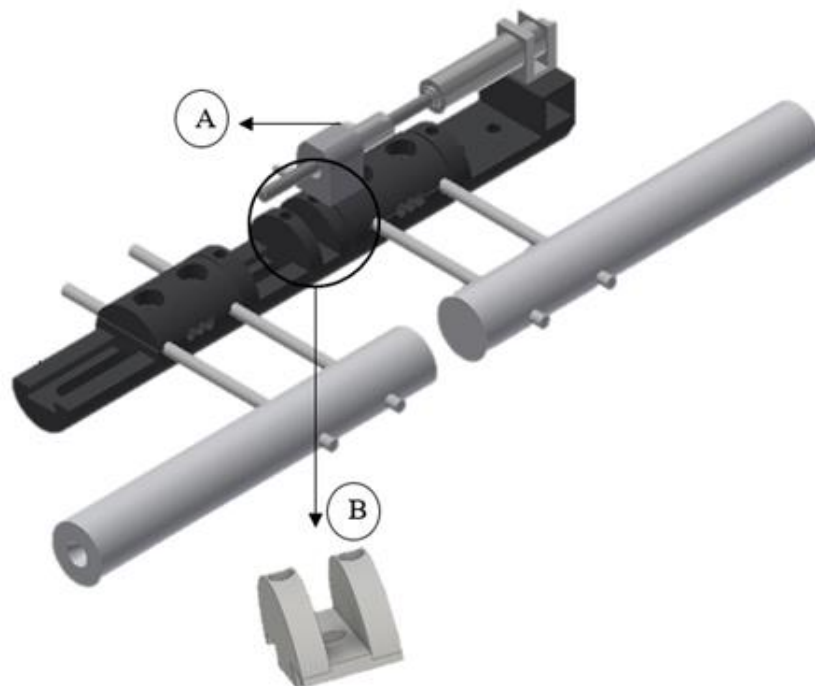
Figure 4.2. Frame of the fixator engaging the spindle drive. Safety clamp (B) detail.
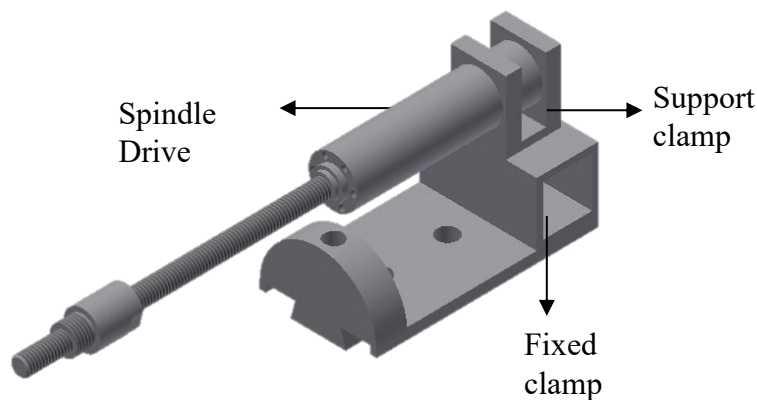
Figure 4.3. Components designed to support the spindle drive.
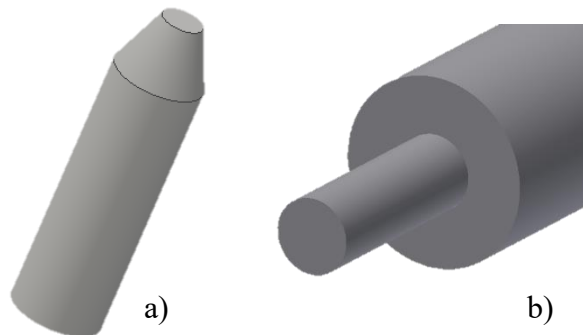
Figure 4.4. a) Support component; b) Detail of the support plus nylon tube.

4.2.1.   Numerical study – preliminary analysis

The model of finite elements was implemented in the software ADINA® considering tetrahedral 3D-Solid elements with 8 nodes per element and 3 degrees of freedom per node for all the models that were simulated regarding the present dissertation.

The materials used were all modelled as homogenous and isotropic each one with different mechanical properties. Whereas the frame of the fixator was considered as Aluminium Alloy 7075 T6 with a Young's modulus of 70 GPa and a Poisson's ratio of 0.33, both nylon tubes were modelled with a Young's modulus of 3 GPa and a Poisson's ratio of 0.39. Due to being stainless steel, the spindle was modelled as homogenous and isotropic

with a Young's modulus of 200 GPa and a Poisson's ratio of 0.29 and the standard nut of bronze was modelled with a Young's modulus of 121 GPa and a Poisson's ratio of 0.34.

The dimension of the elements ranged from 0.1 mm to 3 mm which corresponds to a total of 192412 elements.

The contact surfaces are of the type 3D-Contact and are all *Tied* with the exception of two contact groups which were defined as *Not Tied.* These contact groups connect the surface between the standard nut and the spindle and then the bottom surfaces of the sliding clamp and the top surfaces of the rail.

Boundary conditions were fixed at the bottom surface of the lower nylon tube and in one of the surfaces of the safety clamp. The load type was selected as Pressure which was being applied at the circular surface of the nylon which has an area of 594 mm^2.

Figure 4.5 presents the mesh that was used in this analysis, differentiating the components that were attributed with *Not Tied* contacts. It also represents the boundary conditions, loading and mesh that was utilized in preliminary analysis.

Afterwards, some improvements were made in the simulation regarding boundary conditions and loading applications. Two supports were added to the structure in order to make contact with the nylon tubes, as seen in Figure 4.6. The lower surface of support 1 is fixed on all degrees of freedom and the side surfaces of the support 2 are fixed on x-axis and z-axis, allowing movement only on y-axis. In the simulations with these improvements, the load is applied on the top surface of support 2, which as an area of 113.1 mm^2. The contact surfaces between the nylon tubes and the supports were considered *Not Tied.*

The boundary conditions and load for this model with the first components and improvements can be seen in Figure 4.6. With these new components, the simulation ran with a total of 197275 elements.
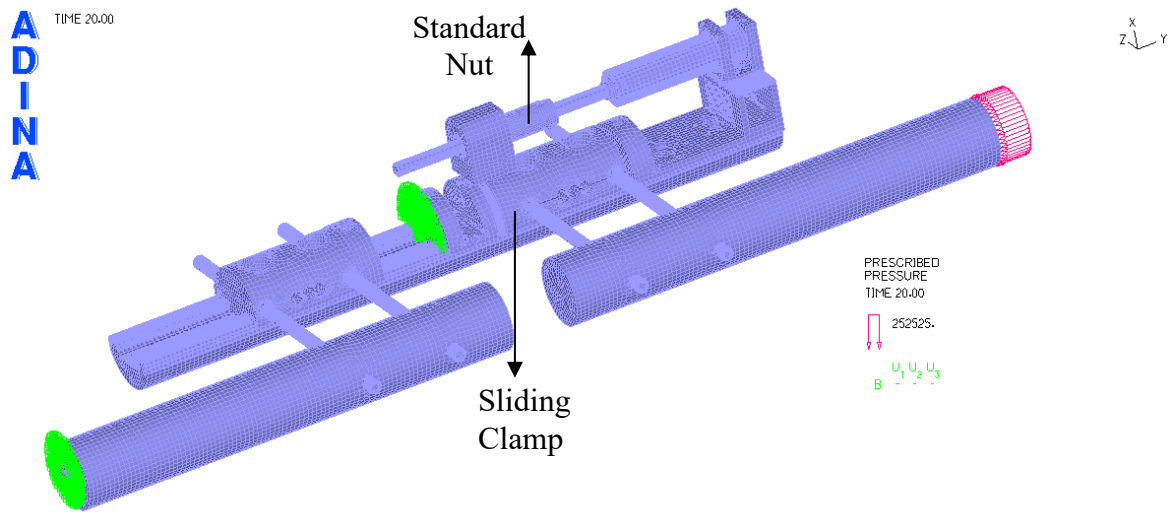
Figure 4.5. Boundary and loading conditions. Visualization of the mesh.
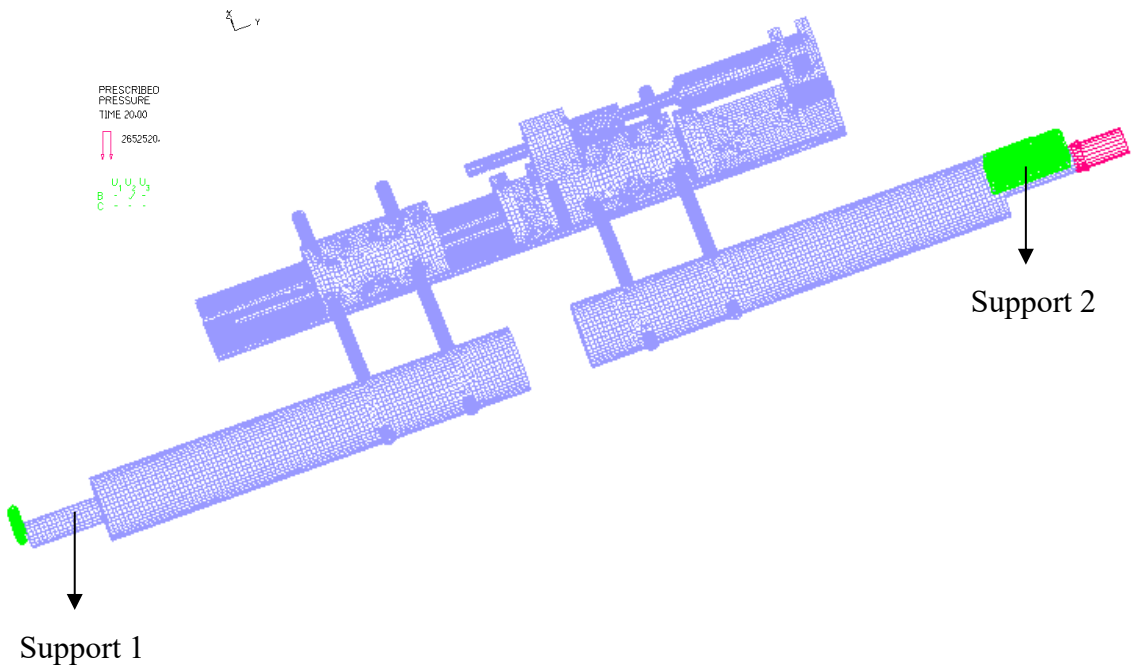
Figure 4.6. Improvements in boundary conditions and loading applications.

4.3. New components

Having received the spindle, a few problems arose, namely the fact that the first designed support became unviable due to the fragility of the extreme part of the spindle. In order to rectify it, two other components were designed and the frame was simplified, having the higher fixed clamp removed. Figure 4.7 shows these new components C and D and Figure 4.8 presents a prototyped box with the aim of protecting the fragile part of the spindle and to store the hardware necessary to achieve and register the micromovements [με]. This box has 64 x 25 x 14 mm as exterior dimensions and is clamped to the component C with three M4 bolts and has a lid in the back for better protection of the equipment. Component D is surrounding the standard nut of the spindle. The lid is secured to the hardware box by four M4 bolts.
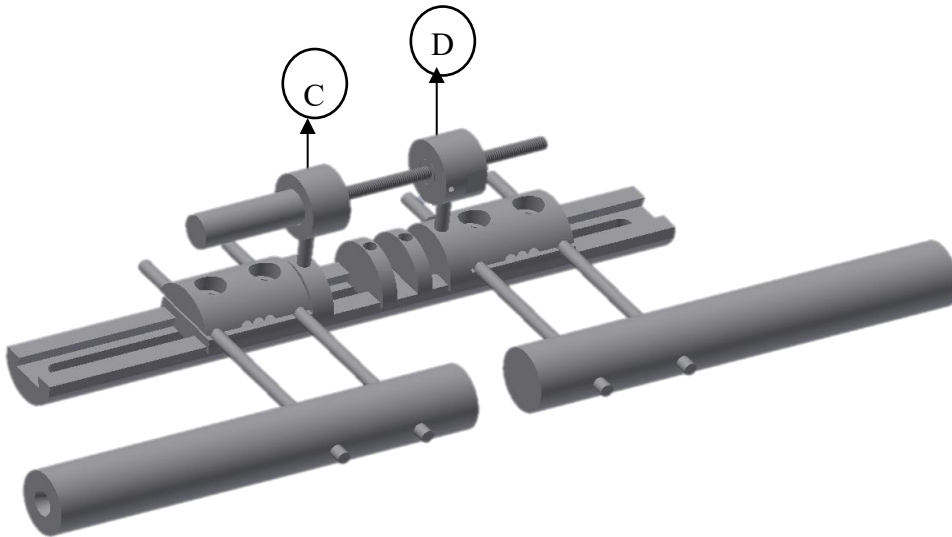
Figure 4.7. Newly designed components.
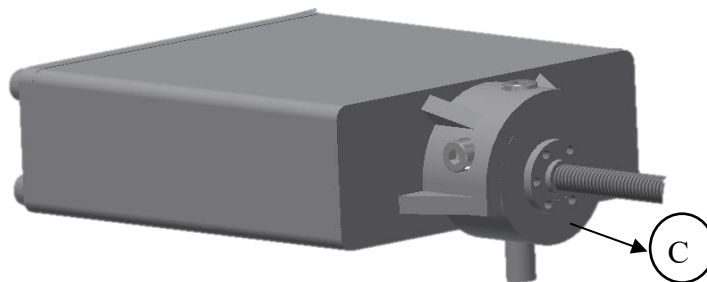
Figure 4.8. Prototyped box and respective lid.

4.3.1. Numerical study

This new numerical model only includes the components C and D, as seen in Figure 4.7, instead of all the components that were designed up to this point. With these new components, the elements of the mesh had its dimension ranging from 1 mm to 2 mm, having a total of 181162 elements.

The boundary and loading conditions for this simulation were the same as detailed in Section 4.1.1. The contact surfaces remains as 3D-Contact being *Not Tied* with the exception of two contact groups, also as detailed in Section 4.1.1. Figure 4.9 represents the model that was simulated under these conditions, with the visualization of the mesh, boundary conditions and application of the loads. Improving the previous model with the supports and different loads and boundary conditions, this new mesh had a total of 186025 elements. The boundary conditions are detailed in section 4.1.1. The mesh can be visualized in Figure 4.10.
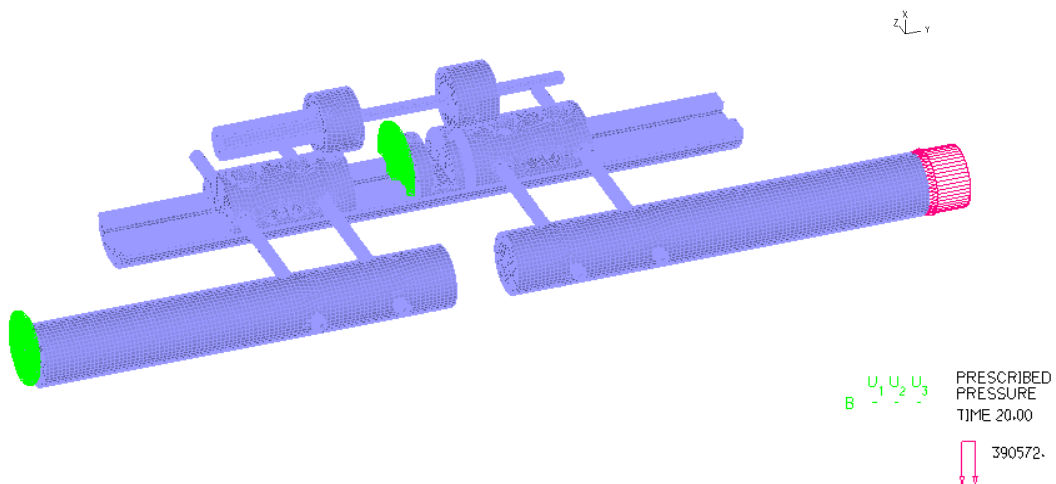
Figure 4.9. Visualization of the mesh with the new components.
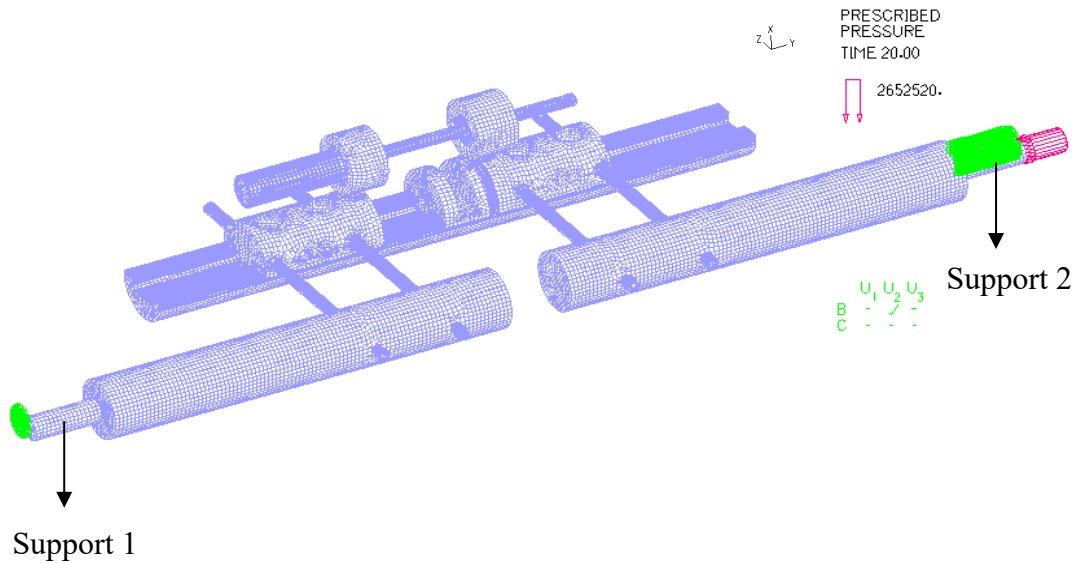
Figure 4.10. Improvements in boundary conditions and loading applications.

4.4. Numerical simulation – validating the tensile test

This last simulation was performed with the intent of numerically validate the results obtained during the tensile test, so it became necessary to replicate the components of the frame, as seen in Figure 3.1, and to add a spring element with a fixed value of stiffness.

The contact groups are mostly considered *Tied* with the exception of the contact between the bottom surface of the mobile clamp and the rail and the contact groups between the supports and the nylon tubes, both of which were considered as *Not Tied*. The supports were added to the model to better replicate the tensile test regarding the initial conditions of the test.

The load cell was developed with the lengths of 100 and 130 mm to represent the stiffness of 1400 and 640 N/mm, respectively. However, when considering the stiffness of only one Carbon Epoxy Composite plate, the value of stiffness is reduced by half. Thus the spring element placed in the numerical simulation is supposed to have a value of stiffness (K) of 700 N/mm and 320 N/mm for lengths of 100 mm and 130 mm, respectively, allowing the validation of the experimental work. However, since this element is connected between

all the 234 nodes of each face of the nylon, the spring has a number of elements equal to 234 and the value of stiffness of each spring becomes the value of K divided by the amount of existing springs.

The loading was considered as the type Pressure and was applied on the top surface of the newly designed support 2. The boundary conditions are detailed in Section 4.1.1.

The dimension of elements used in the simulation ranged from 1 mm to 2 mm, leaving a total of 173393 elements. This mesh can be visualized in Figure 4.11.
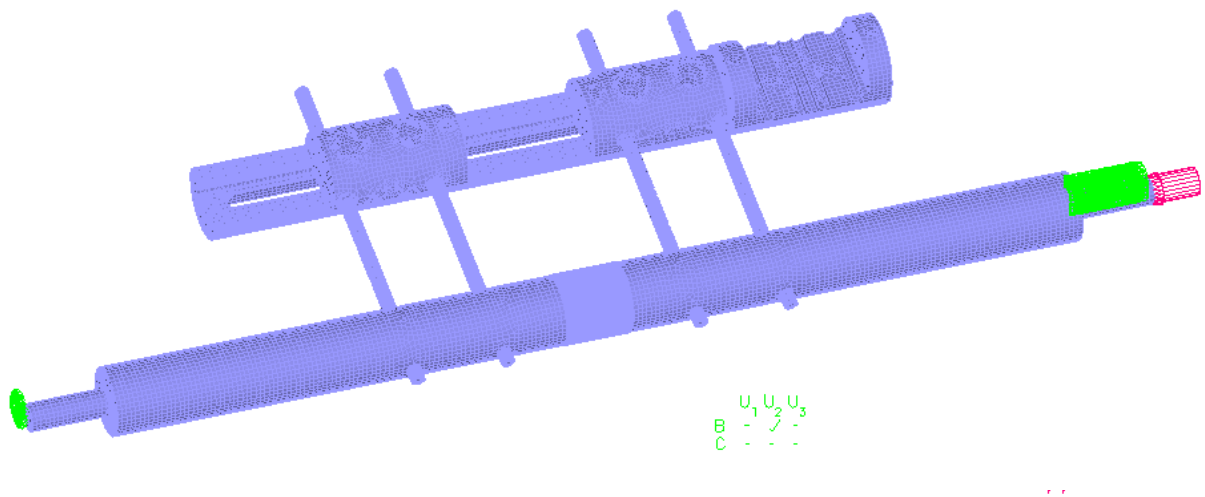
Figure 4.11. Visualization of the mesh, loading and boundary conditions.

5.   ANALYSIS AND DISCUSSION OF RESULTS

This chapter is reserved to the analysis and discussion of the results obtained throughout this dissertation concerning the external fixator with an element of variable stiffness and with an engine that promotes micromovements to the fracture focus.

5.1. Setup considering an element of variable stiffness

As referred in the previous chapter, one of the aims of this dissertation is to evaluate the value of force that goes through the fracture focus and the amount of load that is absorbed by the frame of the fixator, including the nylon tubes and the four pins.

In this section of Chapter 5 it is discussed the results obtained in the calibration procedure of the strain gages as well as the results achieved in the tensile test. This will allow to correlate the weight bearing of the patient with the value of load that takes part in the stimulation of the bone callus.

5.1.1.   Calibration of the strain gages

The data gathered in this experiment was analysed in Microsoft Office Excel and a calibrated equation was determined with both the traction and the compression tests, as seen in Figure 5.1. Equation (5.1) represents the equation of the calibrated line, being y the value of microstrain determined by the strain gages and x the value of weight applied in the nylon tube:

$$y = 4.684x + 4.4837 \tag{5.1}$$

Note that the weights interact directly with the fracture focus since there is no fixator to absorb some of it. Since there is only the nylon tubes and pins, it is correct to assume that the weight that is being applied in the nylon tube is the same weight that presses the composite and promotes the deformation read by the strain gages. By reversing the equation (5.1) a new equation is obtained. This equation (5.2) allows to calculate the value

of load in the fracture focus (P), according to the value of deformation that occurs when there is load being applied in the tensile test. It should be pointed out that the deformation value corresponds to the mean of the four absolute values obtained from the four strain gages.

$$P = \frac{Deformation - 4.4837}{4.684} \tag{5.2}$$
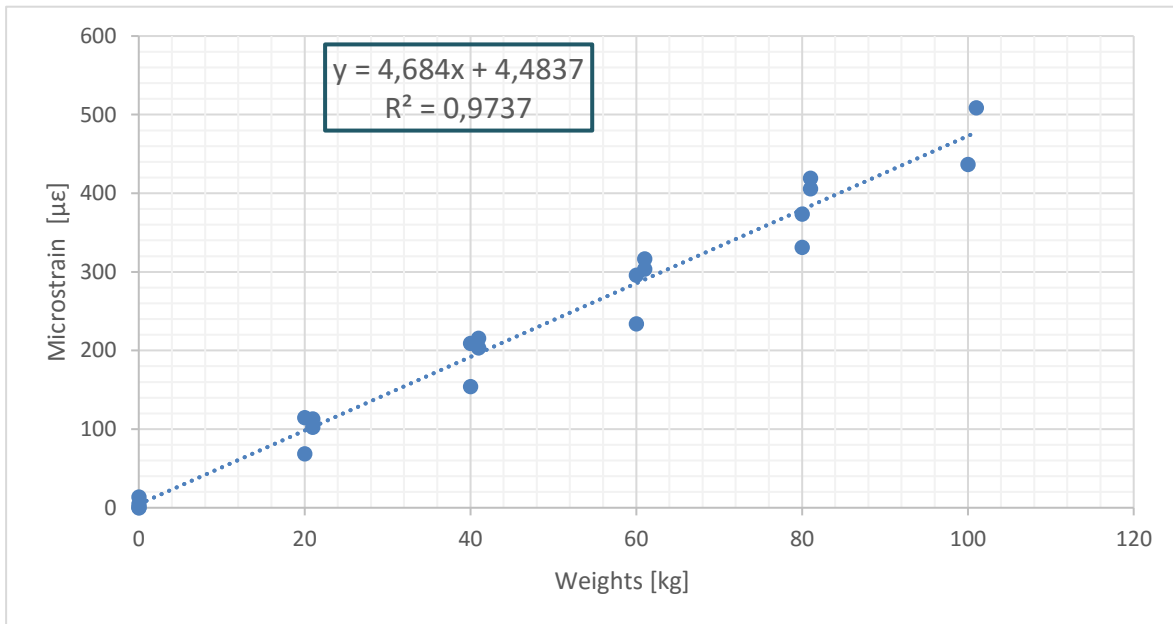
Figure 5.1. Values of deformation obtained for each measured weight.

5.1.2. Tensile test

Since the value of stiffness for the composite with 100 mm of length, of 1400 N/mm, is greater than the value of stiffness for the composite with 130 mm of length, of 640 N/mm, it was expected that the load applied in the tensile test to obtain the same displacement of 1 mm were greater for the composite of 100 mm due to its stiffness and this fact was proved during the test, as seen in Figure 5.2. Note that "c100" and "c130" is meant to represent the composite with 100 mm and 130 mm of length, respectively, and "dist50",

"dist60", "dist70" and "dist80", is meant to distinguish the distance between the axis of the nylon tubes and the frame of the fixator.

The results obtained with a distance between axes of 90 and 100 mm are not presented in Figure 5.2 due to the its small difference regarding the load transfer to the load cell with different lengths of the composite's plates. This shows that, for both these distances, the load cell stiffness does not have significant influence on the behaviour of the fixator.
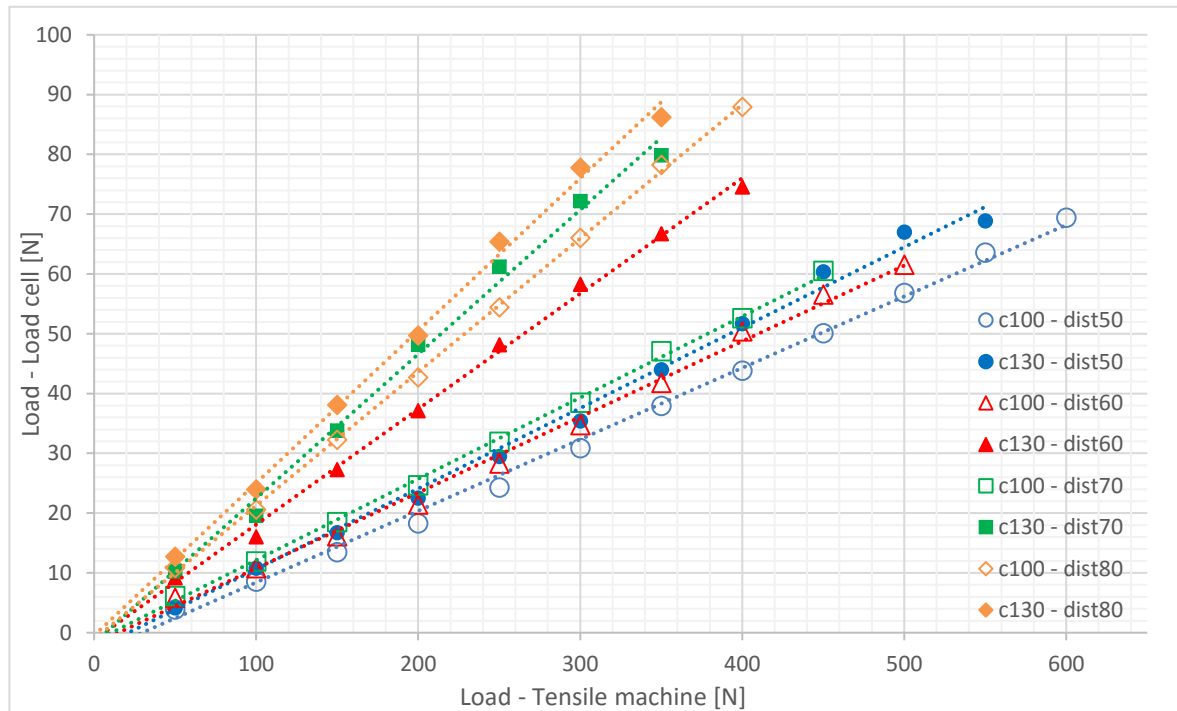
Figure 5.2. Comparison between the load applied in the tensile test and the load read in the load cell for the different values of length of the Carbon Epoxy Composite and different distances between axes.

As seen in Figure 5.2., for the same distance between axes, the value of load being applied by the tensile test decreases once the length of the composite increases to 130 mm. Furthermore, for the same value of the length of the composite, the value of load of the tensile test also decreases once the distance between axes increases. This is due to the fact that the whole structure becomes stiffer once the frame distances itself fewer millimetres from the nylon tubes, in comparison with larger distances.

In Table 5.1 and Table 5.2 are represented the data gathered in this test once the nylon tube achieved the displacement of 1 mm, for a length of Carbon Epoxy Composite of 100 mm and 130 mm, respectively. For the same value of stiffness, when increasing the distance between axes two different conclusions are achieved. Firstly, the value of load in the tensile test decreases and secondly, the value of load read in the load cell increases. Both

of these conclusions are explained due to the distance between the nylon tubes and the frame of the fixator having an effect on the global stiffness of the structure.

For the same value of length of the composite, the whole structure becomes stiffer when decreasing the distance between axes, hence the fact that is necessary to apply more amount of load in the tensile test to obtain the same value of displacement. Moreover, part of the load applied in the tensile test is absorbed by the structure and what remains is transferred to nylon tube and registered by the developed load cell. It was expected that, by having a structure with greater value of stiffness, it would absorb even more load applied in the tensile test and transfer even less to the nylon tubes. In Tables 5.1 and 5.2 is shown that the ratio of load that passes through the nylon tube into the fracture focus increases once decreasing the stiffness of the structure, either by increasing the distance between axes or by varying the stiffness of the Carbon Epoxy Composite. However, this value of ratio is calculated for the value of load that enabled a displacement of 1 mm of the nylon tube. For a better understanding of the load transfer in the structure during the tensile test, the difference between the loads read in the load cell for both lengths of the composite was calculated for each value of load in the tensile test. These results are presented in Tables 5.3 and 5.4 for distances between axes of 70 and 80 mm, respectively, and it shows a different outcome.

Table 5.1. Data obtained for a displacement of 1 mm in the tensile tests with a Carbon Epoxy Composite stiffness of 1400 N/mm.

Length of the composite	100 mm					
Load cell stiffness	1400 N/mm					
Distance between axes	50 mm	60 mm	70 mm	80 mm	90 mm	100 mm
Load (1) – Load cell [N]	69.4	61.6	60.5	87.9	86.8	94.8
Load (2) – Tensile Machine [N]	626.4	521.8	476.6	427.0	393.9	408.6
Ratio (1)/(2)	0.11	0.12	0.13	0.21	0.22	0.23

Table 5.2. Data obtained for a displacement of 1 mm in the tensile tests with a Carbon Epoxy Composite stiffness of 640 N/mm.

Length of the composite	130 mm					
Load cell stiffness	640 N/mm					
Distance between axes	50 mm	60 mm	70 mm	80 mm	90 mm	100 mm
Load (1) – Load cell [N]	68.9	74.5	79.9	86.2	67.1	87.8
Load (2) – Tensile Machine [N]	535.8	384.7	334.5	350.0	232.7	277.9
Ratio (1)/(2)	0.13	0.19	0.24	0.25	0.29	0.32

By calculating the difference between the values of load read in the load cell for a stiffness of 1400 N/mm and 640 N/mm, at the same distance, it becomes clear that the larger difference corresponds to the distance between axes of 70 mm, of 44%. In the tests with larger distances, this difference decreases, as well as the tests with fewer distances. The lower difference, of 14.2%, occurs to the distance between axes of 80 mm.

For small distances between axes, increasing the global rigidity of the structure, the rigidity of the load cell does not have an impact on the results. Furthermore, when increasing the distance between axes further that 70 mm, it can also be observed that the stiffness of the fracture focus does not have influence in the structure. In the tensile test can be observed that the stiffness of the load cell has a larger impact on the whole structure when the distance between axes is of 70 mm.

Tables 5.3 and 5.4 shows the data gathered during the tensile test regarding the load that was read in the load cell for a distance between axes of 70 mm and 80 mm, respectively, when varying the length of the Carbon Epoxy Composite. It is also represented the difference associated with the amount of load read in the load cell for the each composite's length. This difference was calculated having as a reference the values of load obtained with a Carbon Epoxy Composite length of 130 mm. The values registered by the load cell represent the values of load calculated with the equation (5.2), for the correspondent value of deformation obtained in the tensile test. Note that the values obtained were until the nylon reached a displacement of 1 mm in the tensile test.

The tables that present the data of the tensile test regarding the values of load registered by the load cell, and respective differences, for the distance between axes of 50, 60, 90 and 100 mm for a Carbon Epoxy Composite length of 100 and 130 mm are presented in Appendix A.

Table 5.3. Data regarding the tensile test for a distance between axes of 70 mm.

| Machine load [N] | Value of load read in the Load cell [N] | | Difference [%] |
	Carbon Epoxy Composite length: 100 mm	Carbon Epoxy Composite length: 130 mm	
0	-0.833	-0.797	-
50	6.124	10.269	40.36
100	11.923	19.609	39.20
150	18.526	33.842	45.26
200	24.680	48.182	48.78
250	31.938	61.240	47.85
300	38.503	72.200	46.67
350	47.114	79.850	41.00
400	52.629	-	-
450	60.546	-	-
Average	-	-	44.16

Table 5.4. Data regarding the tensile test for a distance between axes of 80 mm.

| Machine Load [N] | Value of load read in the Load cell [N] | | Difference [%] |
	Carbon Epoxy Composite length: 100 mm	Carbon Epoxy Composite length: 130 mm	
0	-0.90	-0.85	-
50	10.87	12.76	14.78
100	20.59	23.99	14.17
150	32.29	38.11	15.26
200	42.74	49.71	14.03
250	54.43	65.39	16.76
300	66.08	77.79	15.05
350	78.27	86.22	9.22
400	87.94	-	-
Average	-	-	14.18

5.2. Setup engaging a spindle drive

The purpose of the simulations being presented in this chapter is to analyse the behaviour of the tibia, through the nylon tubes, in face of roughly 10-20 % of weight bearing of the patient, meaning a load of 300 N being applied in the top surface of the nylon tube. Furthermore, the amount of load necessary to achieve a displacement of 1 mm is also a question that this dissertation aims to contribute. As explained in Chapter 4, these simulations will be made taking in consideration the new components designed to support the spindle.

These simulations are to be a point of reference of the value of load necessary to apply to the engine once the experimental work commences.

5.2.1.   Numerical analysis – preliminary analysis

The first numerical results were obtained with a load of 300 N being applied in the nylon tube. Afterwards, the same model with a load of 150 N was simulated and the y-displacement of the nylon and mobile clamp was analysed for both these loads. Knowing these displacements and loads, the load that promoted a y-displacement of 1 mm in the nylon was determined. Having selected the lower face of the mobile nylon tube and the lower face of the mobile clamp in post-processing, the value of displacement in these two surfaces was listed according to the Table 5.5. Improving the boundary conditions and loading applications as explained in Chapter 4, the new values of displacement of the nylon and mobile clamp were also listed in Table 5.5.

With the first components, the value of load applied in the nylon tube that enabled a displacement of 1 mm was 215 N. With the improvements that were made in the boundary conditions, the model was no longer considered as a rigid body and the load that enabled the same displacement of 1 mm decreased, becoming 118 N.

Table 5.5. Displacement of the nylon and mobile clamp before and after introducing improvements to the model.

| Load [N] | Y – Displacement [mm] | | | |
| | First components | | Improvements regarding loading and boundary conditions | |
	Clamp	Nylon	Clamp	Nylon
300	0.09	1.39	0.96	1.83
150	0.04	0.69	0.67	1.27
215	0.06	1.00	-	-
118	-	-	0.53	1.00

5.2.2. Numerical analysis – new components

The simulations with the new components had the same background as the previous simulations. The first model had a load of 300 N and then of 150 N and after analysing both y-displacements obtained in the nylon tube, the load to achieve a displacement of 1 mm was determined. These data are represented in Table 5.6.

Table 5.6. Displacement of the nylon and mobile clamp before and after introducing improvements to the model.

| Load [N] | Y – Displacement [mm] | | | |
| | New components | | Improvements regarding loading and boundary conditions | |
	Clamp	Nylon	Clamp	Nylon
300	0.48	1.88	1.74	3.01
150	0.20	0.91	0.85	1.47
164	0.23	1.00	-	-
104	-	-	0.58	1.00

Comparing the data obtained for the first components and the new components, it becomes clear that the new components do not had such stiffness to the frame as the first components designed, since the displacement of the clamp's lower surface is higher with the new components and the value of load that enables the displacement of 1mm of the nylon

tube is lower with these new components. The improvements that were made to the models allow the nylon to reach a displacement of 1 mm for lower values of applied load.

Regarding the improvements that were made in the boundary conditions of the model, since it was no longer considered a rigid body, the value of load that enabled a displacement of 1 mm decreased to 104 N instead of the previous 164 N.

Figures 5.3 and 5.4 are referring to the simulation of the new components having a load of 300 N being applied in the nylon tube. As seen in Table 5.6, the displacement of the nylon for this situation is 3.01 mm. In Figure 5.3 can be seen the effect that the load applied on the nylon tube has on the pins and in Figure 5.4 is shown that the maximum displacement occurs on the extremity of the lower pin that is connected to the top nylon tube with a value of 3.13 mm whereas the displacement of the nylon tube remains 3.01 mm. This is due to the bending of the pins during the simulation with this load.

a)   b)
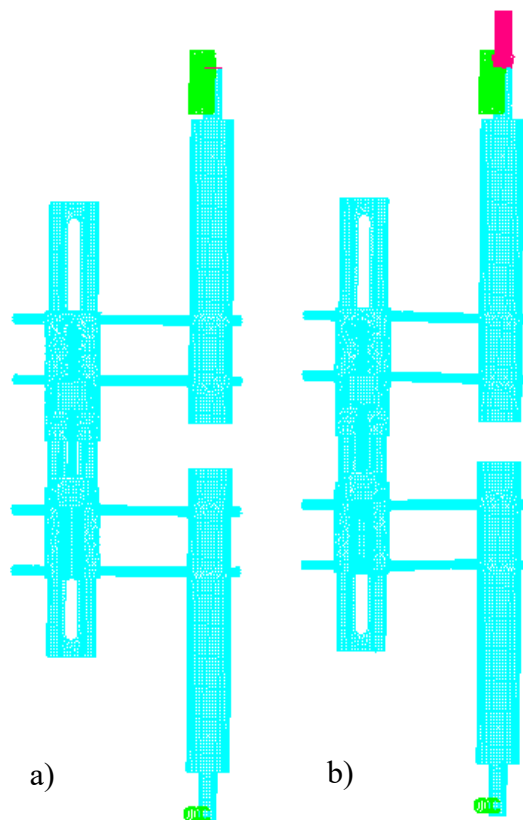
Figure 5.3. Model with the new components: a) before applied load; b) after applied load.
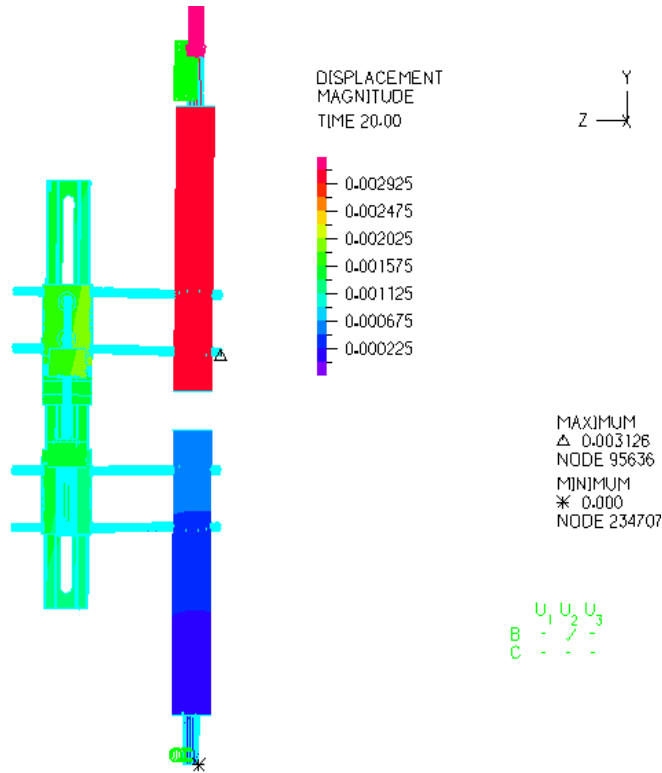
Figure 5.4. Distribution of the displacement magnitude in the model with the new components.

5.2.3. Comparison between the numerical simulation and the tensile test

Having in mind the tensile test that was performed considering the setup with an element of variable stiffness, the numerical simulation allows the validation of the experiment of the tensile test. Table 5.7 represents the data obtained in these simulations. Note that the values of load that were applied in the simulation correspond to the loads that enabled a nylon displacement of 1 mm in the tensile test. The relative error associated with the simulation is also presented in Table 5.7 and was calculated according to the values obtained in the tensile test for the same distance between axes, as seen in Equation (5.3).

$$Error\ [\%] = \frac{Nylon\ displ.(tensile\ test) - Nylon\ displ.(simulation)}{Nylon\ displ.(tensile\ test)} \times 100 \tag{5.3}$$

The model was simulated having a distance between axes of the frame of the fixator and the nylon tubes of 80 mm. The load was type Pressure and was applied in the top surface of support 2.

Table 5.7. Numerical data and error associated with the validation of the tensile test

Load cell Stiffness [N/m]	Load in the tensile machine [N]	Stiffness of each spring [N/m]	Y-Displ. (nylon) [mm]	Y-Displ. (clamp) [mm]	Error [%]
1400×10^3	427	2991.5	0.60	0.43	40.0
640×10^3	350	1367.5	0.89	0.60	10.5

Since there are problems regarding the replication of the tensile test parameters in the numerical simulations, it was expected that the error would be of 10-12%. However, the error of 40 % that occurred for the model with spring elements with 2991.5 N/m was unexpected and can be explained by the area of the support 2, being 113.1 mm^2, which was only an approximation. In fact, the area of the sphere that is subjected to the contact with the nylon during the tensile test is difficult to determine, contributing for the appearance of errors.

In order to reduce the error of these simulations, the area in which the load is applied was reduced to 85 mm^2. This new data is presented in Table 5.8. The error obtained for the model with a spring element of a stiffness of 2991.5 N/m is by default whereas the error for the model with a stiffness of the spring of 1367.5 N/m was by excess.

Table 5.8. Numerical data and error associated with the validation of the tensile test, when modifying the area in which the load is applied.

Load Cell Stiffness [N/m]	Load in the tensile machine [N]	Stiffness of each spring [N/m]	Y-Displ. (nylon) [mm]	Y-Displ. (clamp) [mm]	Error [%]
1400×10^3	427	2991.5	0.80	0.56	20.0
640×10^3	350	1367.5	1.19	0.79	-18.6

6. CONCLUSIONS

The present dissertation had the main purpose of contributing to the development of a system that enabled the acceleration of bone callus formation through the introduction of micromovements into the fracture focus. The external fixator used as a prototype for this dissertation was constituted of a rail, two fixed clamps and a mobile one, four pins and two nylon tubes.

One of the purposes of this work was to study the behaviour of the fixator's frame and determine the amount of load that is transferred to the fracture focus once the nylon was being solicited under compression. For this, it was implemented an experimental methodology taking in consideration the specifications listed in the norm ASTM F 1541-02 that provides a characterization of external skeletal fixation devices.

The tensile machine SHIMADZU model AUTOGRAPH AG-X and a developed load cell was used to monitor the applied loads and displacements and register the test results. The experimental tests enabled the study of the external fixator's behaviour regarding the influence of the stiffness of the fixator on the amount of load that is absorbed by it or transferred to the fracture focus.

The results showed that, for the experimental conditions that were obtained, it was possible to determine the amount of load that was being transferred to the fracture focus during the test performance and register the sensibility of the distance between axes of nylon and fixator. It was observed that this distance influenced the behaviour of the fixator during the test, translating into a variation of the stiffness of the whole structure. From all the distances that were considered, 70 mm was the one which warrants the higher transfer of load into the fracture focus. For distances higher than 70 mm, the influence of the load cell stiffness is not very significant, same as for the distance of 50 mm. Overall, the distances between the axes of the nylon tubes and the fixator's beam of 60 mm and 70 mm are the ones that appear to have more sensibility to the stiffness of the load cell.

The positioning of the fixator, regarding the distance to the bone, can be chosen depending on the patient's stature. According to some specialists, the distances are usually of 80 mm to a grown patient and 50 mm to a child, which can always be adjusted according to their medical needs. Taking this into account, the analysis made in this work becomes

important in order to determine the correct positioning of the fixator regarding the amount of load that is meant to be transferred into the fracture focus.

Another purpose of this dissertation was to study the possibility of introducing micromovements into the fracture focus through an engine with the aim of accelerating bone callus formation. Even though no experimental work with the engine was performed due to the delay of its delivery, numerical models were simulated with the purpose of studying the influence of weight bearing on the displacement of the nylon. Both experimental and numerical work that was developed will be important to understand the value of load necessary to program the hardware to control the engine once this experimental work starts. In the first instance, the models were considered as rigid bodies and the correspondent data was analysed. Afterwards some improvements were made to the models and were simulated, no longer being considered as rigid bodies. The correspondent data was also analysed and its implications discussed. The obtained results and models can be seen as a beginning of the idea in order to implement the control of micromovements based on a micromotor and an electronic control unit.

Furthermore, models were simulated in order to validate the experimental work performed in the tensile test. The error associated with the discrepancies of the results from both the experimental and numerical work was determined. Due to the difficulty to replicate the conditions and parameters of the tensile test, the error was higher than expected.

6.1. Future work

This work was a contribution to the study of the possibility to artificially improve the healing process of bone fractures. Four main domains for future work should be pointed out:

1. Despite new components being designed with the purpose of supporting the engine to the external fixator's frame, it was not possible to do experimental work to accomplish the introduction of micromovements into the fracture focus based on a micromotor and an electronic unit. This is an important outcome for future work;

2. An interesting challenge would also be the experimental study of an optimized distance between the pins and the fracture focus that enables a faster healing response;

3. Since this work optimized the distance between the axes of the frame of the fixator and the nylon tubes, it would be relevant to update the model in the numerical software and analyse the updated data;

4. Finally, it would also be relevant to compare the results obtained with experimental work performed with a synthetic model of the tibia instead of nylon tubes.

BIBLIOGRAPHY

[1]   "Skeletal Systems - Labeled Diagrams of the Human Skeleton," [Online]. Retrieved from https://www.innerbody.com/image/skelfov.html. [Accessed on 15-03-2016, 10:15am].

[2]   M. F. Paulino, "Desenvolvimento de Metodologias de Formação do Calo Ósseo em Fraturas com Tratamento Baseado em Sistemas de Fixação Externa". Projeto Tese DEM-FCTUC, 2014.

[3]   M. M. L. Sá, "Avaliação Experimental de um Sistema Integrado de Fixação Óssea." Dissertação de Mestrado DEM-FCTUC, 2015.

[4]   G. Lowet, X. Dayuan, E. Design, and K. U. Leuven, "Study of the vibrational behaviour of a healing tibia using finite element modelling" J. Biomechanics, 1996. 29(8): p. 1003-1010.

[5]   M. C. Hobatho, R. Darmana, and P. Pastor, "Development of a three-dimensional finite element model of a human tibia using experimental modal analysis," *J. Biomech.*, vol. 24, no. 6, pp. 371–383, 1991.

[6]   AO Foundation, "Müller AO Classification of Fractures – Long Bones," Retrieved from http://www.aofoundation.org/Documents/mueller_ao_class.pdf. [Accessed on 16-03-2016, 11:20am].

[7]   B. D. Browner, "Skeletal Trauma: Basic Science, Management, and Reconstruction," vol. 1, pp. 1–414–1421, 2009.

[8]   M. S. Taljanovic, M. D. Jones, J. T. Ruth, J. B. Benjamin, J. E. Sheppard, and T. B. Hunter, "Fracture fixation," *Radiographics*, vol. 23, no. 6, pp. 1569–1590, 2003.

[9]   D. P. Moss and N. C. Tejwani, "Biomechanics of external fixation: A review of the literature," *Bull. NYU Hosp. Jt. Dis.*, vol. 65, no. 4, pp. 294–299, 2007.

[10]   Pontarelli. R. W., T. Nirmal and D. Polonet, "External Fixation of Tibial Fractures," *Iowa Orthop. J.*, vol. 2, pp. 80–88, 1982.

[11]   R. Littlewood, "The Benefits and Risks of the Ilizarov Technique for Limb Reconstruction" [Online]. Retrieved from http://www.ouh.nhs.uk/limbreconstruction/information/documents/Ilizarovtechniq ueforlimbreconstruction.pdf. [Accessed on 22-03-2016, 12:40pm]

[12]   D. K. Lee, E. T. A. Duong, and D. G. Chang, "The Ilizarov Method of External Fixation: Current Intraoperative Concepts," *AORN J.*, vol. 91, no. 3, pp. 326–340, 2010.

[13]   "Hybrid Triax External Fixation System" [Online]. Retrieved from http://admin5.mdvan.net/english/07_import/01_catalog_detail.asp?sp_code=C131 1024&full_code=CCC1. [Accessed on 25-03-2016, 3:19pm]

[14] H. Isaksson, "Recent advances in mechanobiological modeling of bone regeneration," *Mech. Res. Commun.*, vol. 42, pp. 22–31, 2012.

[15] Ito, K., Perren, S. M. "Biology of fracture healing" AO Fundation Publishing [Online]. Retrieved from https://www2.aofoundation.org/wps/portal/surgerymobile?contentUrl=/srg/popup/further_reading/PFxM2/12_33_biol_fx_heal.jsp&soloState=precomp&title=&Language=en. [Accessed on 04-04-2016, 4:46pm]

[16] R. D. Burghardt, K. Yoshino, N. Kashiwagi, S. Yoshino, A. Bhave, D. Paley, and J. E. Herzenberg, "Bilateral double level tibial lengthening in dwarfism," *J. Orthop.*, vol. 12, no. 4, pp. 242–247, 2015.

[17] D. C. L. Carvalho, G. C. Rosim, L. O. R. Gama, M. R. Tavares, R. A. Tribiolo, I. R. Santos, and A. Cliquet, "Tratamentos não farmacológicos na estimulação da osteogênese," *Rev. Saude Publica*, vol. 36, no. 5, pp. 647–654, 2002.

[18] A. Goldberg and J. Scott, "Orthofix External Fixation: Basic Considerations," pp. 1–76, 2010.

[19] Goodship, a E., & Kenwright, J. (1985). "The influence of induced micromovement upon the healing of experimental tibial fractures". The Journal of Bone and Joint Surgery. British Volume, vol. 67(4), p. 650–655.

[20] G. A. Ilizarov, "The tension-stress effect on the genesis and growth of tissues: Part II. The influence of the rate and frequency of distraction," *Clin Orthop, Philadelphia*, vol. 239, pp. 263–285, 1989.

[21] T. N. Gardner, M. Evans, and J. Kenwright, "The influence of external fixators on fracture motion during simulated walking," *Med. Eng. Phys.*, vol. 18, no. 4, pp. 305–313, 1996.

[22] T. Yamaji, K. Ando, S. Wolf, P. Augat, and L. Claes, "The effect of micromovement on callus formation," *J. Orthop. Sci.*, vol. 6, no. 6, pp. 571–575, 2001.

[23] J. Kenwright, J. B. Richardson, J. L. Cunningham, S. H. White, a E. Goodship, M. a Adams, P. a Magnussen, and J. H. Newman, "Axial movement and tibial fractures. A controlled randomised trial of treatment.," *J. Bone Joint Surg. Br.*, vol. 73, no. 4, pp. 654–659, 1991.

[24] D. I. S. Wolf, A. Janousek, J. Pfeil, W. Veith, F. Haas, G. Duda, and L. Claes, "The effects of external mechanical stimulation on the healing of diaphyseal osteotomies fixed by flexible external fixation," *Clin. Biomech.*, vol. 13, no. 4–5, pp. 359–364, 1998.

[25] ASTM International, "Standard Specification and Test Methods for External Skeletal Fixation Devices", p1-31.

ANNEX A

Specifications of the engine Spindle Drive GP 16 S.

Spindle Drive GP 16 S Ø16 mm, Metric spindle
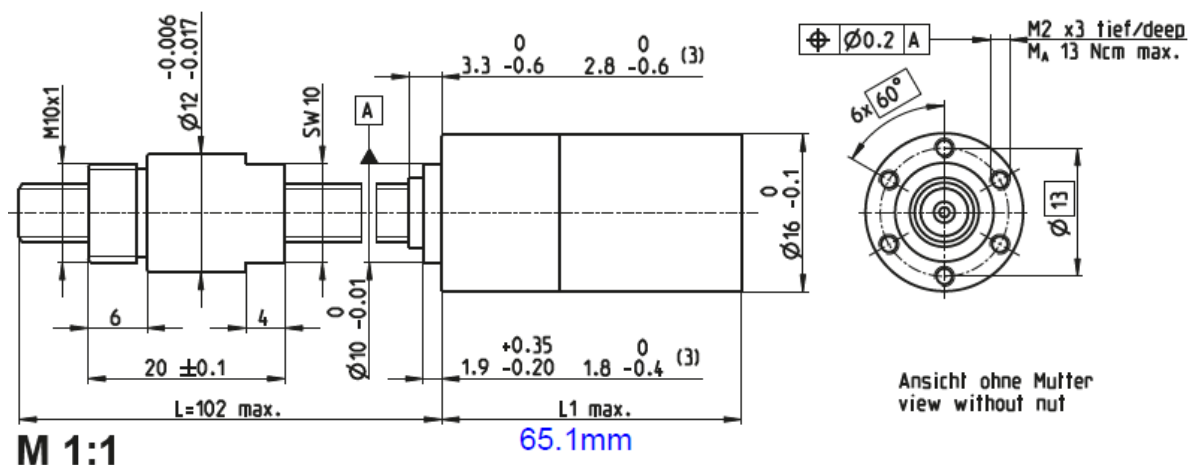
Technical Data

Spindle	M6 x 1, stainless steel
Standard length	102 mm
Special length (5 mm steps)	max. 200 mm
Nut (standard)	thread nut
Material	bronze
Axial play	< 0.134 mm
Planetary gearhead	straight teeth
Bearing	ball bearing/axial bearing
Radial play, 6 mm from flange	< 0.08 mm
Axial play	preloaded
Max. continuous input speed[2]	12000 rpm
Recommended temperature range	-15…+80°C
Max. axial load (static)[1]	500 N

Number of stages	0	1	2	3	4
Max. radial load, 6 mm from flange	20 N	40 N	60 N	80 N	80 N

APPENDIX A

Data obtained by the strain gages concerning the length of the composite being 100 and 130 mm.

Distance between axes: 50 mm

Machine Load [N]	Value of load read in the Load cell [N]		Difference [%]
	Carbon Epoxy Composite length: 100 mm	Carbon Epoxy Composite length: 130 mm	
0.00	-0.96	-0.90	-
50.00	3.88	4.15	6.43
100.00	8.58	10.78	20.46
150.00	13.51	16.76	19.42
200.00	18.29	22.51	18.73
250.00	24.32	29.50	17.55
300.00	30.91	35.43	12.76
350.00	37.95	44.00	13.75
400.00	43.82	51.70	15.24
450.00	50.09	60.37	17.03
500.00	56.85	67.02	15.18
550.00	63.59	68.91	7.72
600.00	69.41	-	-
Average	-	-	14.93

Distance between axes: 60 mm

Machine Load [N]	Value of load read in the Load cell [N]		Difference [%]
	Carbon Epoxy Composite length: 100 mm	Carbon Epoxy Composite length: 130 mm	
0.00	-0.48	-0.78	-
50.00	5.89	9.20	35.96
100.00	10.82	16.03	32.51
150.00	16.16	27.28	40.76
200.00	21.44	37.13	42.26
250.00	28.29	48.18	41.28
300.00	34.75	58.29	40.38
350.00	41.79	66.76	37.39
400.00	50.41	74.54	32.38
450.00	56.58	-	-
500.00	61.58	-	-
Average	-	-	37.87

Distance between axes: 90 mm

| Machine Load [N] | Value of load read in the Load cell [N] | | Difference [%] |
	Carbon Epoxy Composite length: 100 mm	Carbon Epoxy Composite length: 130 mm	
0.00	-0.78	-0.80	-
50.00	12.40	13.64	9.06
100.00	24.73	30.77	19.63
150.00	36.71	50.41	27.19
200.00	49.34	67.09	26.46
250.00	63.64	83.48	23.76
300.00	75.81	-	-
350.00	86.81	-	-
Average	-	-	21.22

Distance between axes: 100 mm

| Machine load [N] | Value of load read in the Load cell [N] | | Difference [%] |
	Carbon Epoxy Composite length: 100 mm	Carbon Epoxy Composite length: 130 mm	
0	-0.584	-0.939	-
50	10.838	15.090	28.18
100	23.835	30.017	20.60
150	36.564	44.801	18.37
200	46.812	60.564	22.71
250	60.982	78.444	22.26
300	70.456	87.767	19.72
350	83.025	-	-
400	94.794	-	-
Average	-	-	21.98